Mycosphere 14(2): 130–157 (2023) www.mycosphere.org ISSN 2077 7019
Article
Doi 10.5943/mycosphere/14/si2/3

Colletotrichum species associated with *Camellia* anthracnose in China

Peng XJ, Wang QC, Zhang SK, Guo K* and Zhou XD*

State Key Laboratory of Subtropical Silviculture, College of Forestry and Biotechnology, Zhejiang A & F University, Hangzhou 311300, Zhejiang, China

Peng XJ, Wang QC, Zhang SK, Guo K, Zhou XD 2023 – *Colletotrichum* species associated with *Camellia* anthracnose in China. Mycosphere 14(2), 130–157, Doi 10.5943/mycosphere/14/si2/3

Abstract

Species of *Camellia oleifera*, *Ca. sinensis* and *Ca. japonica* represent globally-important tree germplasm resource and have significant ecological and economic value. However, they have suffered from anthracnose caused by pathogenic fungi from the genus of *Colletotrichum*. To determine the diversity of *Colletotrichum* species associated with *Camellia* anthracnose in China, we collected infected leaves from three major cultivation provinces. A total number of 167 fungal strains resembling *Colletotrichum* were obtained, 41 from *Ca. oleifera*, 48 from *Ca. sinensis*, and 78 from *Ca. japonica*. Comparison of morphology and phylogenetic analyses based on six loci (ACT, CAL, CHS-1, GAPDH, TUB2 and ITS) of the representative isolates revealed that they fall in four species complexes and represent 15 known and one undescribed taxa. The species complexes are *Colletotrichum gloeosporioides* (*C. aenigma*, *C. alienum*, *C. camelliae*, *C. fructicola*, *C. gloeosporioides*, *C. jiangxiense*, *C. pandanicola*, *C. siamense*, *C. wuxiense* and *C. puerense* described here), *C. acutatum* (*C. fioriniae* and *C. nymphaeae*), *C. boninense* (*C. boninense* and *C. karstii*) and *C. orchidearum* (*C. clivicola* and *C. plurivorum*). Of these, *C. fructicola* was the most dominant species occurring on *Ca. oleifera* (68.3%), *Ca. sinensis* (50.0%) and *Ca. japonica* (29.49%). Pathogenicity test results indicated that *C. camelliae* is the most pathogenic to the three *Camellia* species. This study represents the first report of *C. aenigma*, *C. alienum*, *C. boninense*, *C. camelliae*, *C. clivicola*, *C. fioriniae*, *C. fructicola*, *C. gloeosporioides*, *C. jiangxinse*, *C. karstii*, *C. nymphaeae*, *C. pandanicola* and *C. wuxiense* causing anthracnose on *Ca. japonica* and *C. pandanicola* on *Ca. sinensis*. Knowledge gained in this study enlarges our understanding of *Colletotrichum* species causing anthracnose on three important *Camellia* trees and contributes to the disease management.

Keywords – 1 new species – *Camellia japonica* – fungal diversity – multi-gene phylogeny – pathogenicity

Introduction

Camellia is one of the most traditional and diverse genera within the family Theaceae. It includes at least 280 species, and they are mainly distributed in east Asia (Yang et al. 2011, 2019, Teixeira & Sousa 2021, Talhinhas & Baroncelli 2021). Certain *Camellia* species are of high commercial value. For example, tea-oil tree (*Ca. oleifera*) is China's most important woody oil tree species (Quan et al. 2022). Up till now, its cultivation area has reached close to 5 million ha and the oil production from seeds is around 518,000 tons per year there (State-owned Forest Farms and Nurseries Station, State Forestry Administration of China 2022). *Camellia sinensis* belongs to the

Submitted 18 November 2022, Accepted 2 May 2023, Published 30 May 2023
Corresponding Author: Kai Guo – e-mail – kaiguo@zafu.edu.cn,
Xudong Zhou – e-mail – xudong.zhou@zafu.edu.cn

tea group of *Camellia*, and is a vital beverage tree crop worldwide grown in more than 60 countries (Orrock et al. 2019). Tea leaves are rich in a variety of active substances such as alkaloids, steroids and polyphenols that are beneficial to human health (Anand et al. 2015). *Camellia japonica* is one of the top ten traditional famous flowers in China with great ornamental and medicinal value (Moon & Kim 2018, Zhang et al. 2018). These three *Camellia* species have thus been extensively studied due to their significant economic values (Yang et al. 2018, Teixeira & Sousa 2021, Lin et al. 2022, Zhao et al. 2022). Many species of *Colletotrichum* are fungal pathogens (Van der AA 1978, Liu et al. 2022). They can infect and cause anthracnose in different plant genera including *Camellia*, resulting in serious economic and ecological losses (Guarnaccia et al. 2018, Chen et al. 2021, Zhang et al. 2021, Yang et al. 2022). The disease is more severe and difficult to manage, especially under high temperature and humidity conditions (Zhou et al. 2007, Liu et al. 2009).

Taxonomy of *Colletotrichum* species was confusing as their morphology is similar and there was a lack of comprehensive study using a polyphasic approach to identify the species (Cannon et al. 2014, Talhinhas & Baroncelli 2021). Recently, comparisons of morphological characteristics and multi-gene sequence analyses have been applied to define the taxonomic status in *Colletotrichum*, and a total number of 280 species were clarified (Dowling et al. 2020, Liu et al. 2022). Previous studies reported that there are 11, 16 and three *Colletotrichum* species causing anthracnose on *Ca. oleifera*, *Ca. sinensis* and *Ca. japonica*, respectively (Table 1) (Liu et al. 2015, Hou et al. 2016, Orrock et al. 2019, Li & Li 2020, Wang et al. 2020, Zhang et al. 2021, Li & Li 2022, Peng et al. 2022, Chen et al. 2022). However, there is a lack of comprehensive study on *Colletotrichum* causing anthracnose on the three important *Camellia* species including diversity, occurrence and pathogenicity of pathogens. The aim of this study was thus to achieve these goals using a combined approach of fungal morphology and phylogenetic analyses of multi-locus sequences of ACT, CAL, CHS-I, GAPDH, TUB2, ITS (Weir et al. 2012, Wang et al. 2020, Zhang et al. 2021). The pathogenicity of the representative *Colletotrichum* isolates was further evaluated to contribute to disease management and germplasm selection.

Table 1 *Colletotrichum* species previously reported from *Camellia* anthracnose.

Host	Species	Reference
Ca. oleifera	*C. fructicola*, *C. camelliae*, *C. siamense*, *C. gloeosporioides*, *C. horii*, *C. boninense*, *C. kahawae*, *C. karstii*, *C. fioriniae*, *C. aenigma and C. aeschynomenes.*	Li & Li 2020, Wang et al. 2020, Li & Li 2022, Chen et al. 2022
Ca. sinensis	*C. gloeosporioides*, *C. siamense*, *C. aenigma*, *C. fructicola*, *C. camelliae*, *C. acutatum*, *C. fioriniae*, *C. boninense*, *C. karstii*, *C. truncatum*, *C. cliviae*, *C. crassipes*, *C. jiangxiense*, *C. wuxiense*, *C. henanense* and *C. endophytic*.	Liu et al. 2015, Orrock et al. 2019, Zhang et al. 2021
Ca. japonica	*C. siamense*, *C. aracearum* and *C. camelliae-japonica.*	Hou et al. 2016, Peng et al. 2022

Materials & Methods

Sampling and fungal isolation

Leaves with typical anthracnose symptoms of *Ca. oleifera*, *Ca. sinensis* and *Ca. japonica* plants were collected from the provinces of Zhejiang, Jiangxi, Yunnan and Shanghai in China during the period of 2020-2022. The diseased tissues with black acervuli on the surface were cut into pieces and incubated in moist chambers at 25 °C (Senanayake et al. 2020). The spore mass was collected using a sterile needle under a dissection microscope and the tissues without sporulation were cut into 4-5 mm^2 fragments and surface sterilized with 1% NaClO for 45 s, 75% ethanol for 1 min and rinsed three times in sterile water (Fu et al. 2019). They were transferred onto malt extract agar plates at 25 °C and purified. For further study, pure cultures were stored in 25% glycerol at -80 °C. The specimens were kept at culture collection of tree health division, Zhejiang A&F

University, and ex-type living cultures were deposited in the China General Microbiological Culture Collection Centre (CGMCC), Beijing, China.

DNA extraction, PCR amplification and sequencing

Fungal genomic DNA was extracted using an Ezup Column Fungal Genomic DNA Extraction Kit (Shenggong Bioengineering Co., LTD). Partial regions of six loci were amplified. The partial gene sequence of the actin (ACT) was amplified with primers ACT-512F/ACT-783R (Carbone & Kohn 1999), calmodulin (CAL) with primers CL1C/CL2C (Weir et al. 2012), chitin synthase (CHS-1) with primers CHS-79F/CHS-345R (Carbone & Kohn. 1999), glyceraldehyde-3-phosphate dehydrogenase (GAPDH) with primers GDF1/GDR1 (Templeton et al. 1992), beta-tubulin (TUB2) with primers T1/Bt2b (Glass & Donaldson 1995) and internal transcribed spacer regions and intervening 5.8S nrRNA gene (ITS) with primers ITS4/ITS5 (White et al. 1990). The information on primer pairs used are listed in Table 2.

The PCR amplification was conducted as described by Weir et al. (2012). The PCR amplicons were purified and sequenced at the Qinke Biotech Company, Shanghai, China. The consensus sequences were obtained from forward and reverse sequences with the program SeqMan (DNASTAR, Madison, WI, USA). Sequences generated in this study were deposited in GenBank.

Table 2 Primers used for PCR amplification and sequencing.

Gene	Primer	Primer sequence (5'-3')	Reference
ITS	ITS1	TCCGTAGGTGAACCTGCGG	White et al. (1990)
	ITS4	TCCTCCGCTTATTGATATGC	
ACT	ACT-512F	ATGTGCAAGGCCGGTTTCGC	Carbone & Kohn (1999)
	ACT-783R	TACGAGTCCTTCTGGCCCAT	
TUB2	T1	AACATGCGTGAGATTGTAAGT	Glass & Donaldson (1995), O'Donnell & Cigelnik (1997)
	Bt2b	ACCCTCAGTGTAGTGACCCTTGGC	
GAPDH	GDF	GCCGTCAACGACCCCTTCATTGA	Templeton et al. (1992)
	GDR	GGGTGGAGTCGTACTTGAGCATGT	
CAL	CL1C	GAATTCAAGGAGGCCTTCTC	Weir et al. (2012)
	CL2C	CTTCTGCATCATGAGCTGGAC	
CHS-1	CHS-79F	TGGGGCAAGGATGCTTGGAAGAAG	Carbone & Kohn (1999)
	CHS-345R	TGGAAGAACCATCTGTGAGAGTTG	

Phylogenetic analyses

Sequences of 167 representative isolates were assembled and blasted to investigate their phylogenetic relatives (Dissanayake et al. 2020). The sequences of different gene regions obtained from this study and ex-type cultures downloaded from GenBank were aligned using MAFFT v. 7 online servers (http://mafft.cbrc.jp/alignment/sever/index.html) (Katoh & Standley 2013) and manually adjusted in MEGA v. 7.06 (Kumar et al. 2016). Maximum Likelihood (ML) analysis was performed on the multi-locus alignment using PhyloSuite software v. 1.2.2 (Zhang et al. 2020). Clade stability was assessed in a bootstrap analysis with 1000 replicates. Concatenated analyses of ACT, CHS-1, GAPDH, TUB2 and ITS were conducted for the *C. acutatum* complex and *C. orchidearum* complex (Damm et al. 2012a, Liu et al. 2022), while sequences of ACT, CAL, CHS-1, GAPDH, TUB2 and ITS regions were concatenated for the analysis of the *C. gloeosporioides* complex and *C. boninense* complex (Damm et al. 2012b). PhyloSuite software was used to conduct the statistical selection of best-fit models of nucleotide substitution using the corrected Akaike information criterion (AIC).

The undescribed taxon and its most phylogenetically close neighbors were analyzed using the Genealogical Concordance Phylogenetic Species Recognition (GCPSR) model by performing a pairwise homoplasy index (PHI) test (Quaedvlieg et al. 2014). The PHI test was performed in SplitsTree v. 4.14.6 (Huson & Bryant 2006) to determine the recombination level within

phylogenetically closely related species using a six-locus concatenated dataset (ACT, CAL, CHS-1, GAPDH, TUB2, and ITS). If the resulting pairwise homoplasy index was below a 0.05 threshold ($\Phi w < 0.05$), it was indicative of significant recombination in the dataset. The relationship between closely related species was visualized by constructing a split graph.

Morphology

Mycelial plugs (5 mm) of purified cultures were transferred from the growing edge of 5-d-old cultures to the centre of 9-mm-diameter malt extract agar (MEA, 2%) plates in triplicate at 25 °C. Colony diameters were measured from 3 to 6 days to calculate mycelial growth rates (mm/d). Colony color, size and density were also recorded.

The shape, color and size of conidia, conidiophores and ascospores were observed using a Carl Zeiss Imager A2 microscope after ten days of cultivation. Sizes of 30 conidia were measured unless no spores were produced. Appressoria were induced by dropping a conidial suspension (10^6 conidia/mL; 50 μL) on a concavity slide containing moistened filter papers with distilled sterile water, and then incubating at 25 °C in the dark. After 24 h to 48 h, the conidial appressoria formed at the ends of germ tubes were measured (Tan et al. 2022).

Pathogenicity tests

Sixteen representative isolates of *Colletotrichum* species were selected for the pathogenicity test on detached leaves of *Ca. oleifera*, *Ca. sinensis* and *Ca. japonica* plants under controlled conditions. The pathogenicity test was conducted with an aliquot of spore suspension (1.0×10^6 conidia per mL) on detached healthy leaves of three hosts in eight replicates each. The healthy-looking leaves were collected and washed three times with sterile water, and air-dried on sterilized filter paper. The leaves are inoculated using the wound/drop inoculation method (Aiello et al. 2015, Cristóbal-Martínez et al. 2017). The 10 μL spore suspension was inoculated on the left side of a leaf after wounding once by pin-pricking with a sterilized needle (insect pin, 0.5 mm diam), an equal amount of sterile water on the right side of the same leaf in parallel as a control. The inoculated leaves were kept in a growth chamber with 85% relative humidity at 26 °C with a 12/12 h light/dark photoperiod. The length of lesions was measured 14 days after inoculation (Bhunjun et al. 2021).

Results

Fungal isolation

Two hundred thirty-eight isolates resembling *Colletotrichum* were obtained and preliminarily identified based on morphology and ITS sequence data. According to the different sampling sites and hosts, 167 representative isolates were chosen for further detailed analyses. Among them, 41 isolates were from *Ca. oleifera*, 48 from *Ca. sinensis* and 78 from *Ca. japonica*. Our result indicated that *C. fructicola* represents the dominant taxon causing anthracnose in these three-plant species (Fig. 1). The occurrence of other *Colletotrichum* species was summarized in Table 3. In short, we obtained five *Colletotrichum* species from *Ca. oleifera* anthracnose, 14 from *Ca. sinensis* and 14 from *Ca. japonica*, respectively. Among them, *C. clivicola* and *C. aeigma* were isolated only from *Ca. japonica*, while *C. puerense* and *C. plurivorum* only from *Ca. sinensis*.

Table 3 *Colletotrichum* species previously reported from *Camellia* anthracnose.

Species	**Occurrence rate (%) on *Ca. oleifera***	**Occurrence rate (%) on *Ca. sinensis***	**Occurrence rate (%) on *Ca. japonica***
C. fructicola	68.3	50.0	29.5
C. siamense	14.6	8.3	23.1
C. camelliae	2.4	8.3	11.5
C. fioriniae	12.2	2.1	7.7
C. wuxiense	2.4	2.1	1.3

Table 3 Continued.

Species	Occurrence rate (%) on *Ca. oleifera*	Occurrence rate (%) on *Ca. sinensis*	Occurrence rate (%) on *Ca. japonica*
C. alienum	-	2.1	6.4
C. boninense	-	2.1	1.3
C. clivicola	-	-	1.3
C. jiangxiense	-	4.2	1.3
C. karstii	-	2.1	3.8
C. aenigma	-	-	1.3
C. pandanicola	-	2.1	3.8
C. nymphaeae	-	4.2	1.3
C. plurivorum	-	4.2	-
C. gloeosporioides	-	4.2	6.4
C. puerense	-	4.2	-

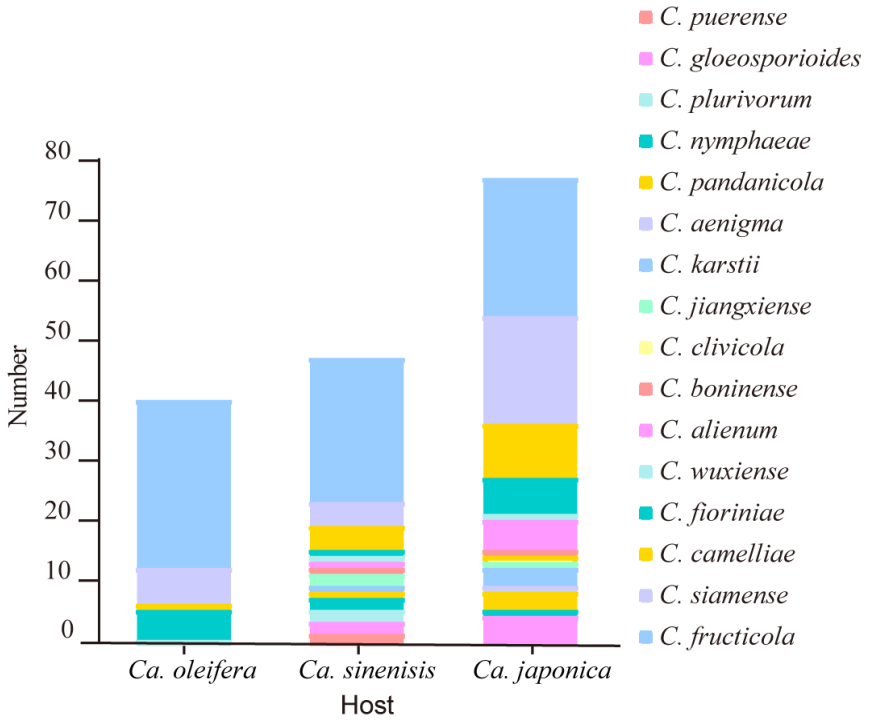

Figure 1 – Occurrence of *Colletotrichum* species causing *Camellia* anthracnose.

Phylogenetic analyses

The 167 representative isolates from three *Camellia* plant species were subjected to multi-locus phylogenetic analyses with concatenated ACT, CAL, CHS-1, GAPDH, TUB2, and ITS sequences for those belonging to the species complexes of *C. gloeosporioides* and *C. boninense*, and concatenated ACT, CHS-1, GAPDH, TUB2, and ITS sequences for *C. acutatum* and *C. orchidearum* species complexes. The results showed that isolates clustered together with 15 known species in four *Colletotrichum* species complexes, including *gloeosporioides* (143 isolates), *acutatum* (15), *orchidearum* (3), and *boninense* (6) (Figs 2–4). In the phylogenetic tree constructed for the isolates in the *C. gloeosporioides* complex, 143 isolates clustered in ten clades corresponding to *C. aenigma* (1), *C. alienum* (6), *C. camelliae* (14), *C. fructicola* (75), *C. gloeosporioides* (7), *C. jiangxiense* (3), *C. pandanicola* (4), *C. siamense* (28), *C. wuxiense* (3). Noticeably two isolates (YNS-22, YNS-30) clustered distantly from any known species in the complex, is herein described as a new taxon, namely *C. puerense* based on the guidelines established in Chethana et al. (2021) and Jayawardena et al. (2021) (Fig. 2). From15 isolates in the *C. acutatum* species complex, 12 isolates grouped in the clade of *C. fioriniae*, and three isolates

were clustered with *C. nymphaeae*. From three isolates in the *C. orchidearum* complex, two isolates clustered with *C. plurivorum* and one with *C. clivicola* (Fig. 3). From *C. boninense* complex, four isolates clustered with *C. karstii*, and two with *C. boninense* (Fig. 4).

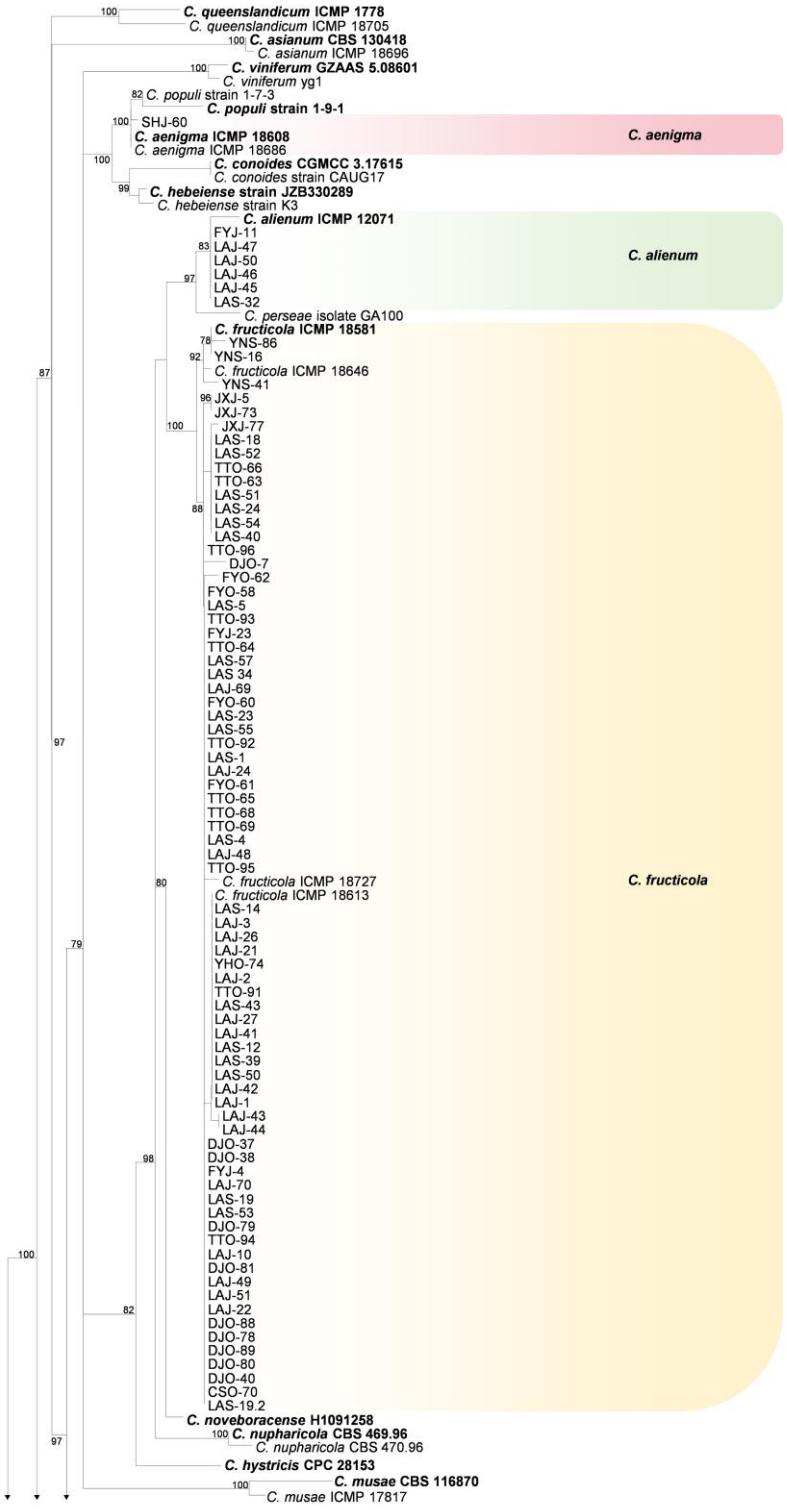

Figure 2 – Phylogenetic tree using sequences of 143 *Colletotrichum* isolates from *Ca. oleifera*, *Ca. sinensis* and *Ca. japonica* leaves in the *C. gloeosporioides* complex. The species *C. boninense* (CBS 123755) was selected as an outgroup. The tree was built using concatenated sequences of the ACT, CAL, CHS-1, GAPDH, TUB2, and ITS gene regions. Bootstrap values >50% (1000 replication) are given at the nodes. Ex-type or reference cultures are in bold. Colored blocks indicate clades containing isolates from *Camellia* plants.

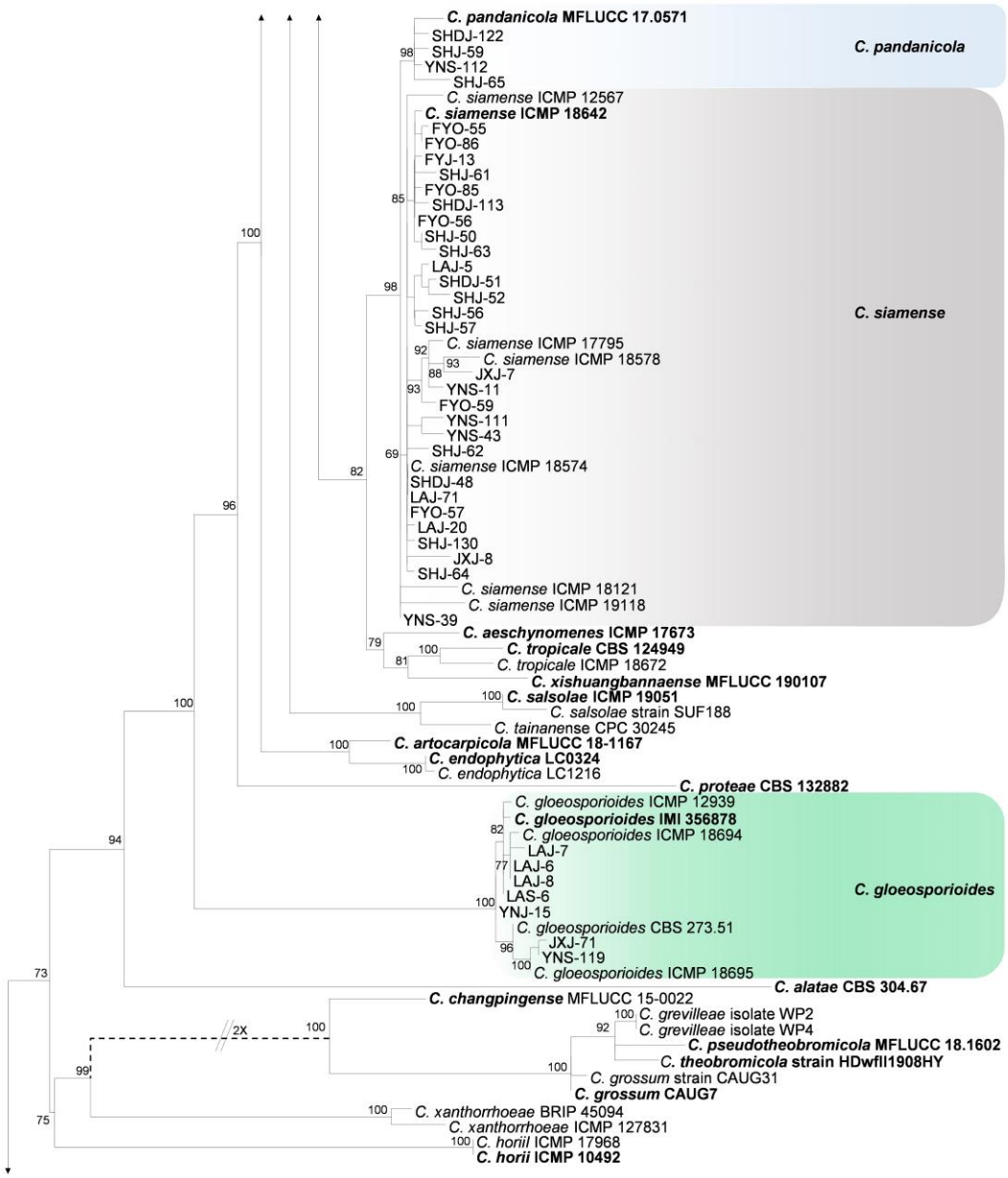

Figure 2 – Continued.

Morphological investigation

Cultures of the representative isolates were selected to observe their morphological characteristics. Few differences in colony morphology were obviously observed among the 16 species (Figs 6–21). When grown on MEA, all selected isolates firstly developed white colonies. They became gray-green to black after 7 days except those belonging to *C. acutatum* complex usually appear pink. Abundant orange conidial masses were often observed on the center of the colonies of *C. fructicola*, *C. gloeosporioides*, *C. siamense*, *C. karstii*, *C. fioriniae* and *C. nymphaeae*. A significant difference in growth rate across 16 *Colletotrichum* species was observed (Table 4). The average mycelial growth rate of *C. gloeosporioides* was the fastest, with an average of 11.87 ± 0.4 mm/d. The average mycelial growth rate of *C. fructicola* was 13.6 ± 0.6 mm/day (n = 11), followed by *C. siame*nse (11.0 ± 0.9 mm/d), *C. alienum* (10.7 ± 0.6 mm/d) and *C. fructicola* (10.6 ± 0.6 mm/d), while *C. fioriniae* and *C. nymphaeae* in the *C. acutatum* complex showed the slowest growth rate with 8.2-8.3 mm/d. However, there were no significant differences in the conidial size among the species.

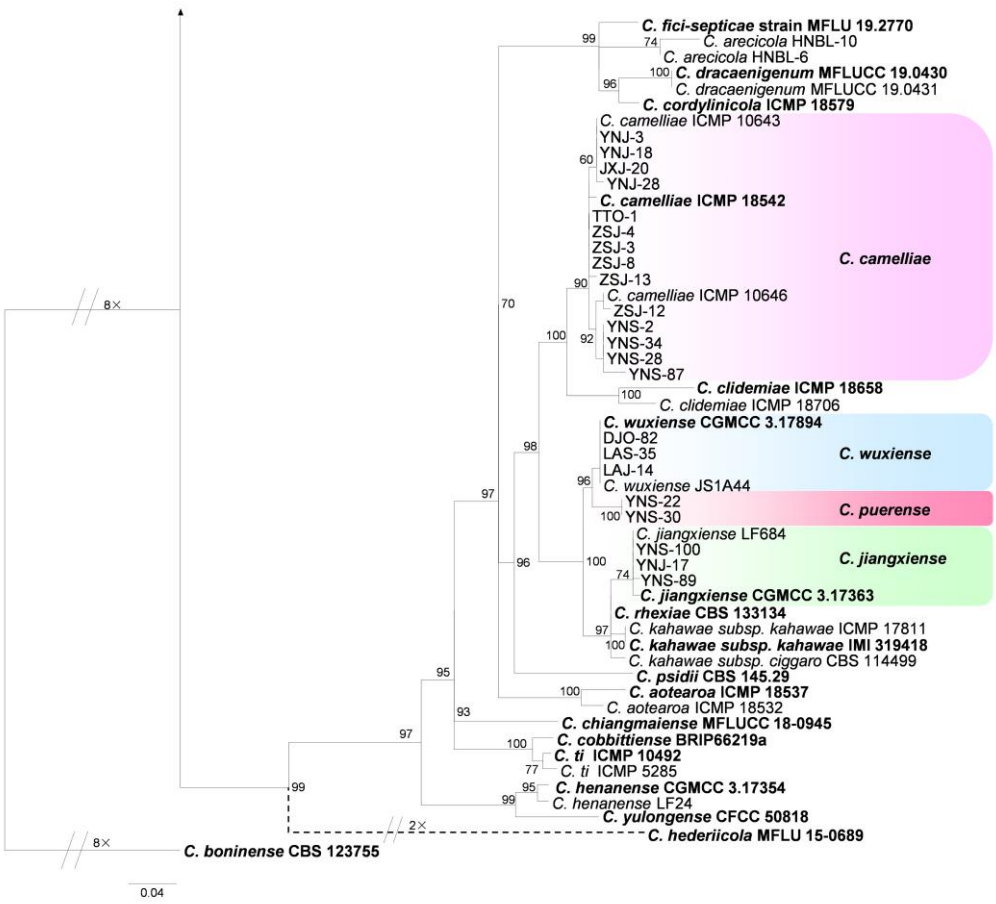

Figure 2 – Continued.

Taxonomy

Based on morphology and multi-locus sequence data, a total of 167 obtained isolates were assigned to 16 *Colletotrichum* species. Of these, one species represents an undescribed taxon and is described below. Species descriptions were also provided for those existing ones according to the complex they reside.

Colletotrichum aenigma Weir & Johnst, Studies in Mycology 73: 135. 2012 Fig. 6

Materials examined – China, Shanghai City, on leaves of *Ca. japonica*, Mar. 2022.

Notes – *Colletotrichum aenigma* belongs to the gloeosporioides species complex and has been recorded as a pathogen on *Ca. sinensis* in China (Wang et al. 2016). This is the first report of *C. aenigma* causing anthracnose on *Ca. japonica* in China.

Colonies diam on MEA attained 70–71 mm in 6 d at 25 °C with entire margin, aerial mycelium sparse, surface white. The conidia are bigger than those of the ex-type isolate (ICMP 18608) 14.4–16.1 × 5.1–6.1 μm, mean ± SD = 15.3 ± 0.8 × 5.6 ± 0.5 μm, L/W ratio = 2.7 vs 12–16.5 × 5–7.5 μm, mean = 14.5 × 6.1 μm, L/W ratio = 2.4 of *C. aenigma*.

Colletotrichum alienum Weir & Johnst, Studies in Mycology 73: 135. 2012 Fig. 7

Materials examined – China, Zhejiang province, Fu yang City, on leaves of *Ca. japonica*, Mar. 2022; Zhejiang province, Lin'an City, on leaves of *Ca. japonica*, Sep. 2021; Zhejiang province, Lin'an City, on leaves of *Ca. sinensis*, Dec. 2021.

Notes – *Colletotrichum alienum* belongs to the gloeosporioides species complex. The species is known from many important crops such as *Camellia sinensis*, *Diospyros kaki* and *Grevillea* sp.

(Weir et al. 2012, Liu et al. 2013). This is the first report of *C. alienum* causing anthracnose on *Ca. japonica* in China.

Colonies diam on MEA attained 65–67 mm in 6 d at 25 °C with entire margin, aerial mycelium dense, surface greyish-green and reverse dark grey. Conidia (14.8–17.6 × 4.8–5.6 µm, mean ± SD = 16.2 ± 0.8 × 5.2 ± 0.8 µm, L/W ratio = 3.1) are slightly shorter than those of the ex-type isolate (ICMP 12071) 15.5–17.5 × 5–5.5 µm, mean = 16.5 × 5.0 µm, L/W ratio = 3.3 of *C. alienum*.

Colletotrichum boninense Moriwaki, Toy. Sato & Tsuki, Mycoscience 44: 48. 2003 Fig. 8

Materials examined – China, Yunnan province, Pu'er City, on leaves of *Ca. sinsensis* and *Ca. japonica*, Mar. 2022.

Notes – *Colletotrichum boninense* belongs to the boninense species complex. This is the first report of *C. boninense* causing anthracnose on *Ca. japonica* in China. Colonies diam on MEA attained 55–58 mm in 6 d at 25 °C, aerial mycelium sparse, surface light pink. Conidia hyaline, smooth walled, cylindrical, one end rounded and one end slightly acute, 11.5–15.5 × 6.5–7.8 µm, mean ± SD = 14.2 ± 1.2 × 6.5 ± 0.5 µm, L/W ratio = 2.2. The L/W ratio measured here is smaller than described (2.3).

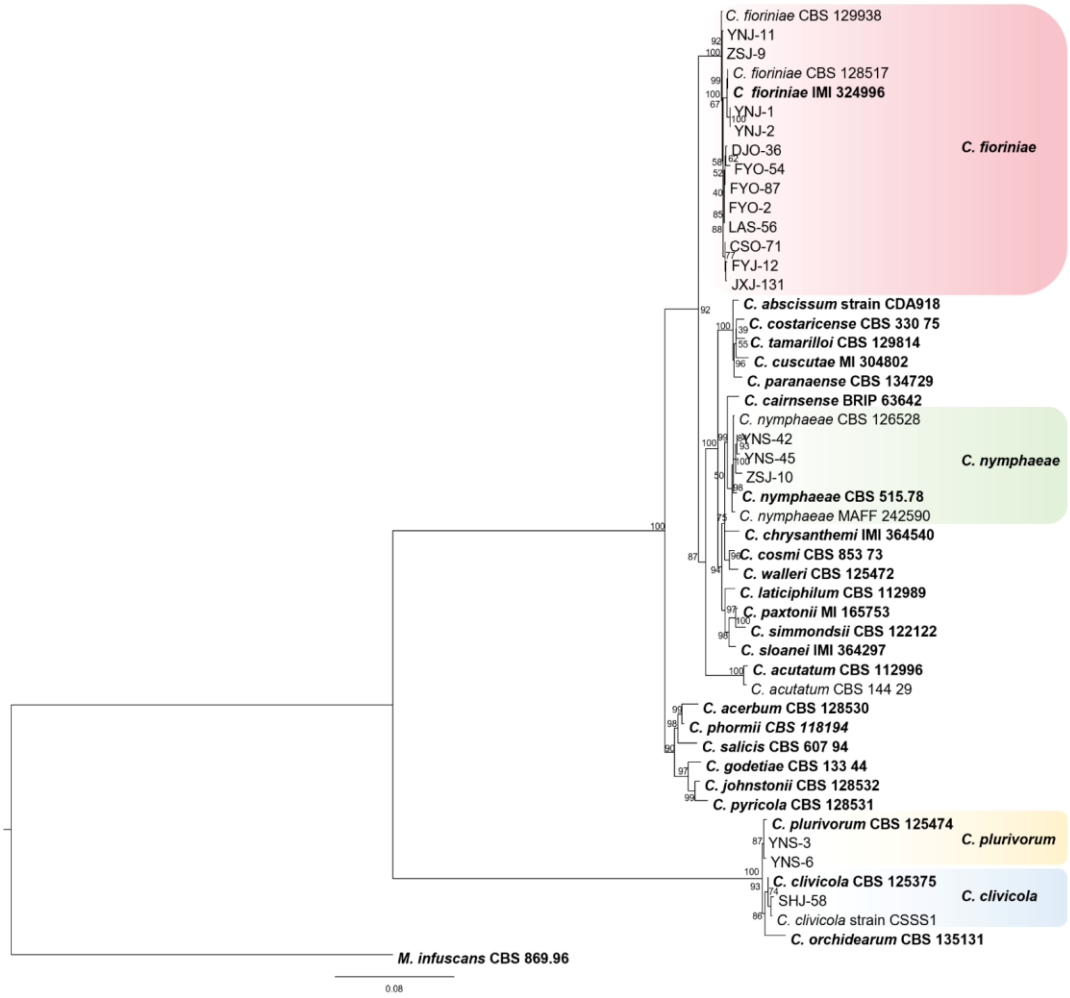

Figure 3 – Phylogenetic tree using sequences of 15 *Colletotrichum* isolates in *C. acutatum* complex and three in *C. orchidearum* complex. The species *Monilochaetes infuscans* (CBS 869.96) was selected as an outgroup. The tree was built using concatenated sequences of the ACT, CHS-1, GAPDH, TUB2, and ITS gene regions. Bootstrap values > 50% (1000 replication) are given at the nodes. Ex-type cultures are in bold. Colored blocks indicate clades containing isolates from *Camellia* plants.

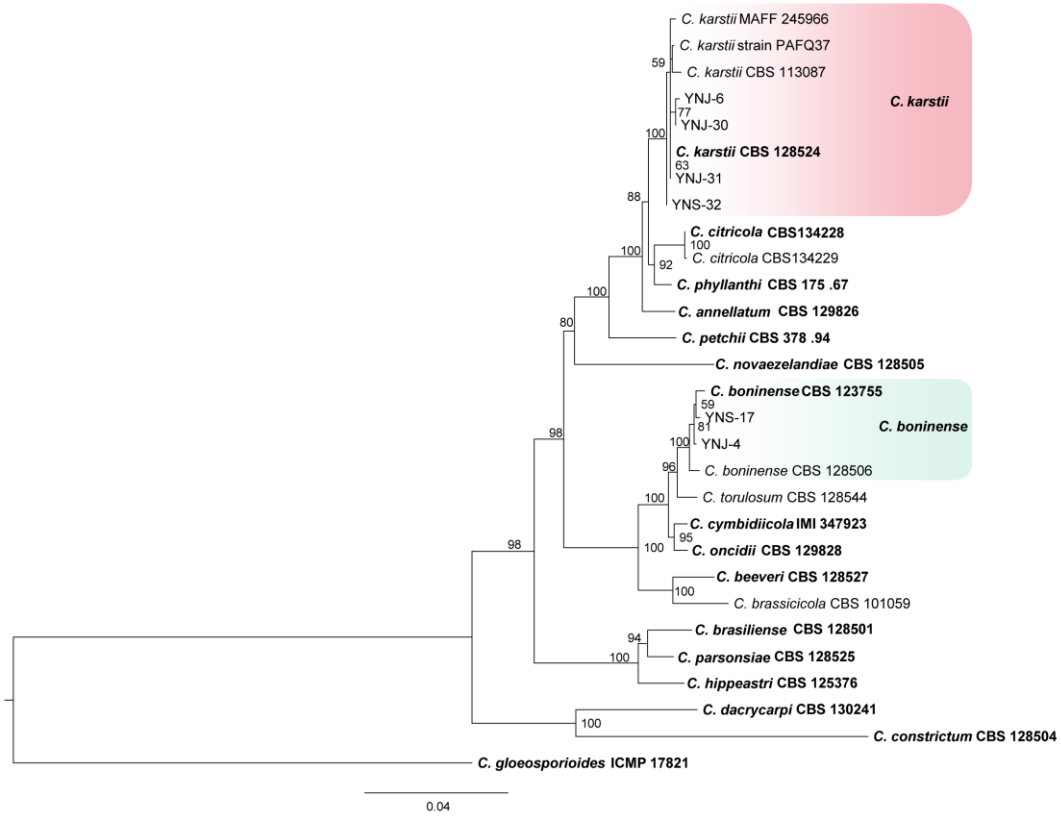

Figure 4 – Phylogenetic tree using sequences of 6 *Colletotrichum* isolates in *C. boninense* complex. The species *C. gloeosporioides* (IMI 356878) was selected as an outgroup. The tree was built using concatenated sequences of the ACT, CAL, CHS-1, GAPDH, TUB2, and ITS gene regions. Bootstrap values > 50% (1000 replication) are given at the nodes. Ex-type cultures are in bold. Colored blocks indicate clades containing isolates from *Camellia* plants.

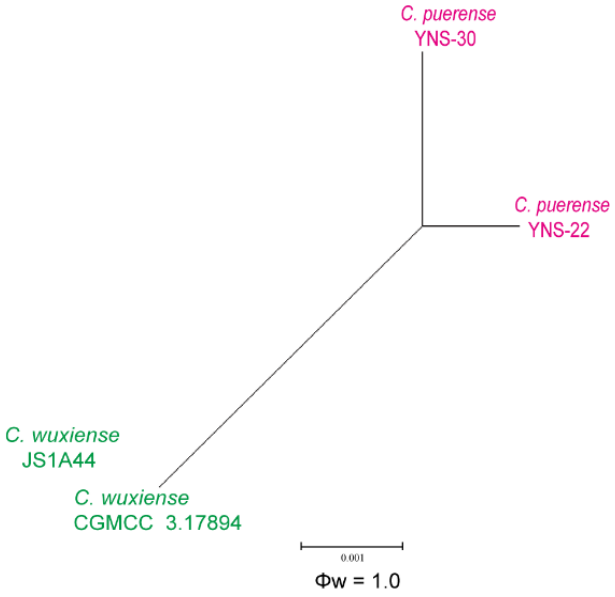

Figure 5 – PHI test of *C. puerense* and phylogenetically related isolates. PHI test value (Φw) < 0.05 indicates significant recombination within the dataset.

Colletotrichum camelliae Massee, Bull. Misc. Inform. Kew: 91. 1899 Fig. 9

Materials examined – China, Yunnan province, Pu'er City, on leaves of *Ca. japonica*, Mar. 2022; Jiangxi province, Ji'an City, on leaves of *Ca. japonica*, Dec. 2021; Zhejiang province,

Zhoushan City, on leaves of *Ca. japonica* and *Ca. oleifera*, Dec. 2021; Yunnan province, Pu'er City, on leaves of *Ca. sinensis*, Dec. 2021.

Notes – *Colletotrichum camelliae* belongs to the kahawae clade within the gloeosporioides complex. The species was first described by Massee on *Ca. sinensis* anthracnose from Sri Lanka (Willis 1899). Our study represents the first report of *C. camelliae* causing anthracnose on *Ca. japonica* in China.

Colonies diam on MEA attained 66–67 mm in 6 d at 25 °C with entire margin, aerial mycelium sparse, surface dark white, cottony, reverse pale-yellow. Conidia hyaline, smooth walled, cylindrical with obtuse ends, 14.2–17.2 × 5–6.5 μm, mean ± SD = 15.7 ± 1.5 × 5.8 ± 0.7 μm, L/W ratio = 2.7. Appressoria brown to black, round or oval.

Colletotrichum clivicola Yan L. Yang, Zuo Y. Liu, K.D. Hyde & L. Cai, in Yang, Liu, Cai, Hyde, Yu & McKenzie, Fungal Diversity 39: 133. 2009 Fig. 10

Materials examined – China, Shanghai City, on leaves of *Ca. japonica*. Mar. 2022.

Notes – *Colletotrichum clivicola* belongs to the orchidearum species complex. This is the first report of *C. clivicola* causing anthracnose on *Ca. japonica* in China.

Colonies diam on MEA attained 67–70 mm in 6 d at 25 °C, aerial mycelium sparse, surface dark white. Conidia hyaline, smooth walled, curved, tapering towards apex and base, 19.4–25.2 × 5.1–7.8 μm, mean ± SD = 22 ± 0.9 × 5.7 ± 0.3 μm, L/W ratio = 3.9. The conidia are slightly bigger than those of the ex-type (CBS 125375) 19.5–24.5 × 4.5–7 μm, mean = 21.8 × 5.7 μm, L/W ratio = 3.8 (Yang et al. 2009). Appressoria brown to dark brown, smooth, irregularly shaped.

Colletotrichum fioriniae (Marcelino & Gouli) R.G. Shivas & Y.P. Tan, Fungal Diversity 39: 117. 2009 Fig. 11

Materials examined – China, Zhejiang province, Fu yang City, on leaves of *Ca. oleifera* and *Ca. japonica*, Mar. 2022; Zhejiang province, Lin'an City, on leaves of *Ca. sinensis*, Dec. 2021; Zhejiang province, Zhoushan City, on leaves of *Ca. japonica*, Dec. 2021; Zhejiang province, Lishui City, on leaves of *Ca. oleifera*, Sep. 2021; Jiangxi province, Ji'an City, on leaves of *Ca. japonica*, Dec. 2021; Yunnan province, Pu'er City, on leaves of *Ca. japonica*, Mar. 2022.

Notes – *Colletotrichum fioriniae* belongs to the acutatum species complex. This is the first report of *C. fioriniae* causing anthracnose on *Ca. japonica* in China.

Colonies diam on MEA attained 44–48 mm in 6 d at 25 °C, aerial mycelium sparse, surface light pink. Conidia hyaline, smooth walled, cylindrical, both ends slightly acute, 11.5–16.1 × 5.8–6.6 μm, mean ± SD = 14.5 ± 0.8 × 5.8 ± 0.5 μm, L/W ratio = 2.5. Appressoria brown to dark brown, smooth, rounded or irregularly shaped.

Colletotrichum fructicola Prihastuti, L. Cai & K.D. Hyde, Fungal Diversity 39: 96. 2009 Fig. 12

Materials examined – China, Zhejiang province, Lin'an City, on leaves of *Ca. japonica*, Sep. 2021; Zhejiang province, Lin'an City, on leaves of *Ca. sinensis*, Dec. 2021; Zhejiang province, Fu yang City, on leaves of *Ca. japonica* and *Ca. sinensis*, Mar. 2022; Zhejiang province, Quzhou City, on leaves of *Ca. oleifera*, Sep. 2021; Zhejiang province, Lishui City, on leaves of *Ca. oleifera*, Sep. 2021; Yunnan province, Pu'er City, on leaves of *Ca. sinensis*, Mar. 2022; Jiangxi province, Ji'an City, on leaves of *Ca. japonica*, Dec. 2021.

Notes – *Colletotrichum fructicola* belongs to the gloeosporioides complex. The species is the most dominant *Colletotrichum* species on *Camellia* with a total of 75 isolates. This is the first report of *C. fructicola* causing anthracnose on *Ca. japonica* in China.

Colonies diam on MEA attained 65–68 mm in 6 d at 25 °C, flat with entire margin, aerial mycelium dense, surface light green to gray-green. Conidia hyaline, smooth walled, cylindrical, ends rounded, 15–18.5 × 4.0–7.2 μm, mean ± SD = 15.2 ± 1.5 × 4.6 ± 0.9 μm, L/W ratio = 3.3. The conidia of *C. fructicola* are larger than those of ex-type (MFLU 090228) 9.7–14 × 3–4.3μm, mean = 11.53 × 3.55 μm, L/W ratio = 3.2.

Colletotrichum gloeosporioides (Penz.) Penz. & Sacc., Atti Inst. Veneto Sci. lett., ed Arti, Sér. 6(2): 670. 1884 Fig. 13

Materials examined – China, Zhejiang province, Lin'an City, on leaves of *Ca. japonica*, Sep. 2021; Zhejiang province, Lin'an City, on leaves of *Ca. sinensis*, Dec. 2021; Yunnan province, Pu'er City, on leaves of *Ca. sinensis* and *Ca. japonica*, Mar. 2021; Jiangxi province, Ji'an City, on leaves of *Ca. japonica*, Dec. 2021.

Notes – *Colletotrichum gloeosporioides* belongs to the gloeosporioides complex. This is the first report of *C. gloeosporioides* causing anthracnose on *Ca. japonica* in China.

Colonies diam on MEA attained 71–73 mm in 6 d at 25 °C, flat with entire margin, aerial mycelium dense, surface gray-green. Conidia hyaline, smooth walled, cylindrical, ends bluntly rounded, 14.2–19.3 × 5.2–7.2 μm, mean ± SD = 14.5 ± 1.5 × 5.4 ± 0.5 μm, L/W ratio = 2.7. Appressoria oval or irregular, brown to black, crenate or slightly lobed at edge.

Colletotrichum jiangxiense F. Liu. & L. Cai, Persoonia 35: 82. 2015 Fig. 14

Materials examined – China, Yunnan province, Pu'er City, on leaves of *Ca. sinensis* and *Ca. japonica*, Mar. 2021.

Notes – *Colletotrichum jiangxiense* belongs to the gloeosporioides complex.This is the first report of *C. jiangxiense* causing anthracnose on *Ca. japonica* in China.

Colonies diam on MEA attained 70–71 mm in 6 d at 25 °C, flat with entire margin, aerial mycelium dense, surface white. Conidia hyaline, smooth walled, cylindrical, ends bluntly rounded, 13.2–19.5 × 4.5–6.2 μm, mean ± SD = 15.2 ± 1.2 × 5.2 ± 0.5 μm, L/W ratio = 2.9. The conidia are similar with those of the ex-type isolate (CGMCC 3.17363) 15.2 ± 1.0 × 5.2 ± 0.4 μm, mean = 15.2 × 5.2 μm, L/W ratio = 2.9 of *C. jiangxiense*.

Colletotrichum karstii Y.L.Yang, Zuo Y. Liu, K.D. Hyde & L. Cai, Cryptogam Mycology 32(3): 241. 2011 Fig. 15

Materials examined – China, Yunnan province, Pu'er City, on leaves of *Ca. sinsensis* and *Ca. japonica*. Mar. 2022.

Notes – *Colletotrichum karstii* belongs to the boninense species complex. This is the first report of *C. karstii* causing anthracnose on *Ca. japonica* in China.

Colonies diam on MEA attained 65–67 mm in 6 d at 25 °C, aerial mycelium sparse, surface dark white. Conidia hyaline, smooth walled, cylindrical, one end rounded and one end slightly acute, 13.4–15.5 × 5.6–6.8 μm, mean ± SD = 14.8 ± 0.9 × 6.3 ± 0.3 μm, L/W ratio = 2.3. Appressoria brown to dark brown, smooth, rounded or irregularly shaped.

Colletotrichum nymphaeae Van der Aa, European Journal of Plant Pathology 84(3): 109-115. 1978 Fig. 16

Materials examined – China, Zhejiang province, Zhoushan City, on leaves of *Ca. japonica*, Dec. 2021; Yunnan province, Pu'er City, on leaves of *Ca. sinsensis*. Sep. 2021.

Notes – *Colletotrichum nymphaeae* belongs to the acutatum species complex. This is the first report of *C. nymphaeae* causing anthracnose on *Ca. japonica* in China.

Colonies diam on MEA attained 49–50 mm in 6 d at 25 °C, aerial mycelium sparse, surface light pink. Conidia hyaline, smooth walled, cylindrical, one end rounded and one end slightly acute, 14.8–17.6 × 4.8–5.6 μm, mean ± SD = 15.2 ± 0.9 × 5.3 ± 0.5 μm, L/W ratio = 2.8. Appressoria dark brown, smooth, rounded or irregularly shaped.

Colletotrichum pandanicola Tibpromma & K.D. Hyde, MycoKeys 33: 25. 2018 Fig. 17

Materials examined – China, Zhejiang province, Lin'an City, on leaves of *Ca. japonica*, Sep. 2021; Shanghai City, on leaves of *Ca. japonica*, Mar. 2022; Yunnan province, Pu'er City, on leaves of *Ca. sinensis*. Sep. 2021.

Notes – *Colletotrichum pandanicola* belongs to the gloeosporioides complex. This is the first report of *C. pandanicola* causing anthracnose on *Ca. sinensis* and *Ca. japonica* in China.

Colonies diam on MEA attained 62–65 mm in 6 d at 25 °C, flat with entire margin, aerial mycelium abundant, cottony, surface white. Conidia hyaline, smooth walled, cylindrical, ends rounded or one end slightly acute, 16.1–19.1 × 5–6.3 μm, mean ± SD = 17.3 ± 1.1 × 5.7 ± 0.4 μm, L/W ratio = 3.0.

Colletotrichum plurivorum Damm, Alizadeh & Toy. Sato, Studies in Mycology 92: 31. 2019 Fig. 18

Materials examined – China, Yunnan province, Pu'er City, on leaves of *Ca. sinensis*. Mar. 2022.

Notes – *Colletotrichum plurivorum* belongs to the orchidearum species complex.

Colonies diam on MEA attained 62–64 mm in 6 d at 25 °C, aerial mycelium sparse, surface dark white. Conidia hyaline, smooth walled, straight cylindrical, both ends bluntly rounded, 15.2–17.5 × 5.2–5.8 μm, mean ± SD = 15.8 ± 0.8 × 5.5 ± 0.3 μm, L/W ratio = 2.9. The conidia are slightly smaller than those of the ex-type (CBS 125474) 15–17 × 5.5 μm, mean = 16.0 ± 0.9 × 5.6 ± 0.1 μm, L/W ratio = 2.9 (Damm et al. 2019).

Colletotrichum puerense Peng XJ & Zhou XD, sp. nov. Fig. 19

Etymology – Referring to the tree host from which the fungus was isolated.

Type – China, Yunnan Province, Pu'er City, on leaves of *Ca. sinensis*, Mar. 2022.

Sexual morphs were not observed. Asexual morphs developed on PDA. Vegetative hyphae were hyaline, smooth-walled, septate and branched. Setae not observed. Conidiomata acervular, yellow to light brown, conidiogenous cells were cylindrical to clavate, 9.5–15.2 × 3.5–5 μm, opening 1.5–2.5 μm. Conidia were smooth-walled, aseptate, cylindrical, both ends rounded, contents granular, 17–21 × 4–6 μm, mean ± SD = 19.1 ± 1.8 × 4.6 ± 0.6 μm, L/W ratio = 4.2. Appressoria were dark brown, irregular, often square to ellipsoid in outline, the margin lobate, 6–12 × 6–8 μm, mean ± SD = 8.9 ± 1.2 × 7± 0.5 μm, L/W ratio = 1.3.

Culture characteristics – Colonies diam on MEA attained 58–60 mm in 6 d at 25 °C with entire margin, aerial mycelium dense, surface grey-white with white margin; reverse pale yellow.

Notes – *Colletotrichum puerense* is phylogenetically closely related to *C. wuxiense* CGMCC 3.17894 and *C. wuxiense* JS1A44 (Fig. 2), However, *C. puerense* differs from the latter in ACT (with 98.83% sequence identity), CAL (100%), CHS-1 (99.52%), GAPDH (100%), TUB2 (99.31%) and ITS (99.62%) sequences. Moreover, *C. puerense* has larger conidia (YNS-22, 17–21 × 4–6 μm, mean ± SD = 19.1 ± 1.8 × 4.6 ± 0.6 μm) than those of *C. wuxinese* (mean = 16.9 × 5.5 μm). The PHI test (Φw = 1.0) detected no significant recombination between the isolates and *C. wuxiense* CGMCC 3.17894 and *C. wuxiense* JS1A44 (Fig. 5).

Colletotrichum siamense Prihastuti, L. Cai & K.D. Hyde, Fungal Diversity 39: 98. 2009 Fig. 20

Materials examined – China, Zhejiang province, Fu yang City, on leaves of *Ca. oleifera* and *Ca. japonica*, Mar. 2022; Zhejiang province, Lin'an City, on leaves of *Ca. japonica*, Sep. 2021; Shanghai City, on leaves of *Ca. japonica*, Mar. 2022; Yunnan province, Pu'er City, on leaves of *Ca. sinensis*, Mar. 2022; Jiangxi province, Ji'an City, on leaves of *Ca. japonica*, Dec. 2021.

Notes – *Colletotrichum siamense* belongs to the gloeosporioides complex. The species has been recorded as a pathogen on a wide range of hosts (Weir et al. 2012) and is the dominant species on *Camellia* in this study.

Colonies diam on MEA attained 68–70 mm in 6 d at 25 °C, flat with entire margin, aerial mycelium dense, cottony, surface white. Conidia hyaline, smooth walled, cylindrical, ends rounded, 14.8–17.5 × 5.1–6.3 μm, mean ± SD = 15.5 ± 1.1 × 5.2 ± 0.5 μm, L/W ratio = 3.0. The conidia are bigger than those of the ex-type isolate (CGMCC 3.17363) 15.2 ± 1.0 × 5.2 ± 0.4 μm, mean = 15.2 × 5.2 μm, L/W ratio = 2.9 of *C. siamense*.

Colletotrichum wuxiense Y.C. Wang, X.C. Wang & Y.J. Yang, Scientific Reports 6: 8. 2016

Fig. 21

Materials examined – China, Zhejiang province, Lin'an City, on leaves of *Ca. oleifera* and *Ca. japonica*, Sep. 2021; Zhejiang province, Lin'an City, on leaves of *Ca. sinensis*, Dec. 2021.

Notes – *Colletotrichum wuxiense* belongs in the gloeosporioides species complex. This is the first report of *C. wuxiense* causing anthracnose on *Ca. japonica* in China.

Colonies diam on MEA attained 62–63 mm in 6 d at 25 °C, aerial mycelium dense, surface dark white or olive green. Conidia hyaline, smooth walled, cylindrical, ends rounded or one end slightly acute, 15.2–18.5 × 4.5–6.5 μm, mean ± SD = 15.5 ± 1.2 × 5.5 ± 0.5 μm, L/W ratio = 2.8. Appressoria dark-brown, irregular in shape.

Pathogenicity test

Sixteen representative strains of *Colletotrichum* species were selected for pathogenicity test on detached leaves of *Ca. oleifera*, *Ca. sinensis* and *Ca. japonica*. Under wounded conditions, all strains were pathogenic and infected leaves developed necrotic lesions at 14 dpi (Fig. 22). Diseased lesion lengths varied among the species and hosts (Fig. 23). There were significant differences ($P < 0.05$) of pathogenicity among the 16 species, using the test of least significant difference. Clearly, *C. camelliae* JXJ-20 showed the strongest pathogenicity on three *Camellia* plants, followed by *C. aenigma* SHJ-60, *C. jiangxiense* YNJ-17 and *C. alienum* FYJ-11, and the lesion diameters range from 5.12 mm to 25.67 mm. The other species such as *C. gloeosporioides* LAS-6, *C. pandanicola* SHJ-65, *C. siamense* LAJ-20, *C. wuxiense* LAJ-14, *C. puerense* YNS-22, *C. fioirniae* YNJ-1, *C. nymphaeae* YNS-42, *C. boninense* YNJ-4, *C. karstii* YNS-32, *C. clivicola* SHJ-58 and *C. plurivorum* YNS-6 showed weak pathogenicity with lesion diameters ranging from 3.06 mm to 1.35 mm. Noticeably, pathogenicity of the *C. camelliae* JXJ-20 to three *Camellia* detached leaves significantly varied. Species of *C. pandanicola* SHJ-65 and *C. clivicola* SHJ-58 were almost nonpathogenic to *Ca. sinensis* (1.33 mm–1.35 mm). No lesions were observed in controls.

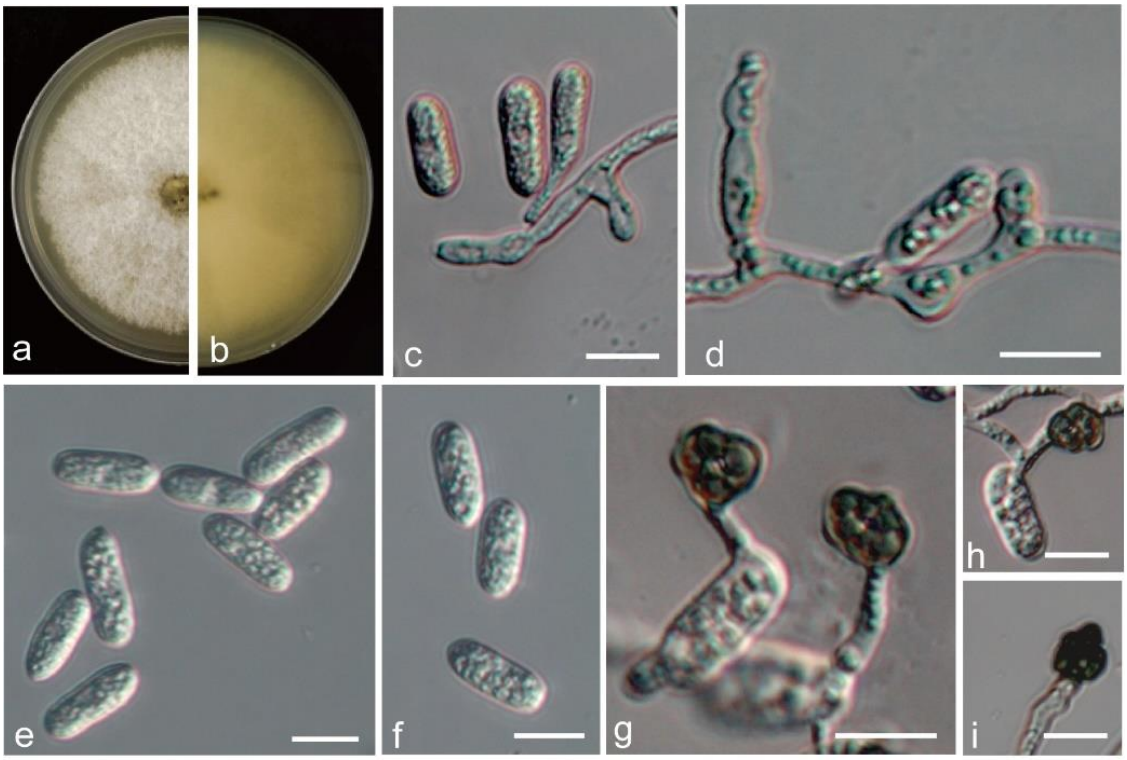

Figure 6 – Morphological characteristics of *C. aenigma*. a Front views of 6-d-old MEA culture. b Back views of culture. c-d Conidiophores. e-f Conidia. g-i Appressoria. a-i Isolate YNS-6. Scale bars = 10 μm.

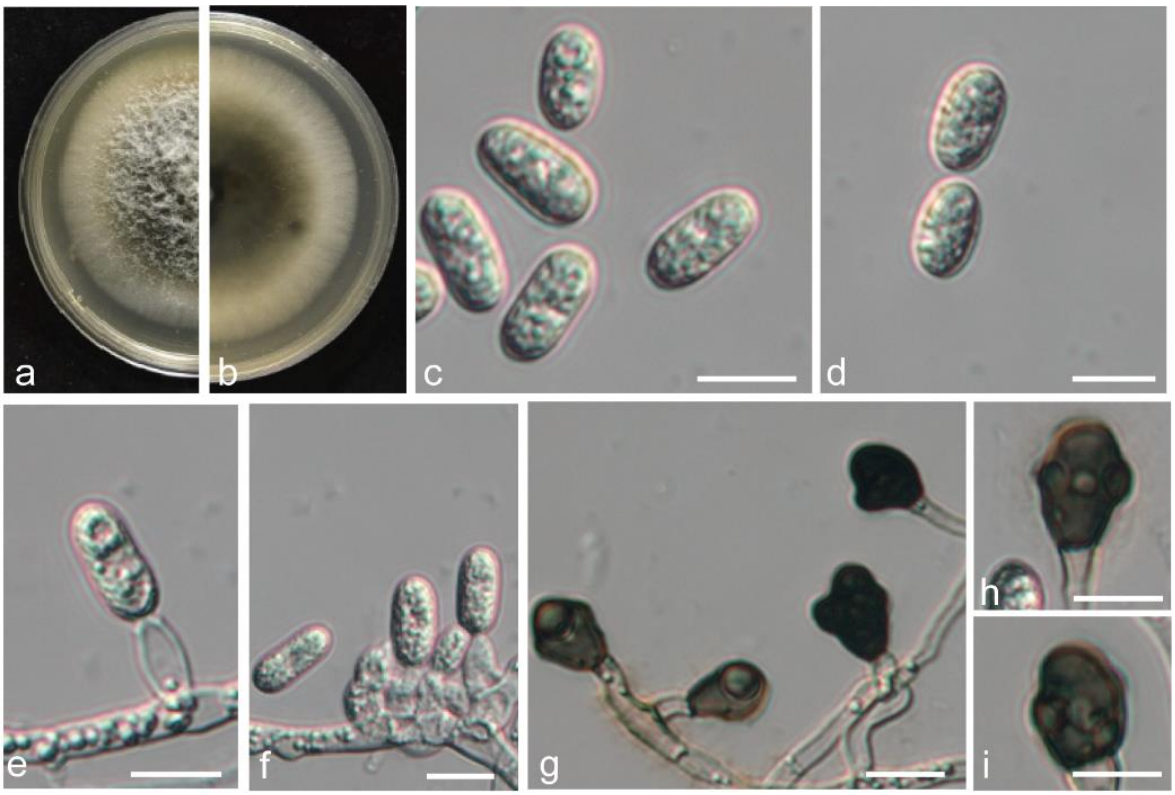

Figure 7 – Morphological characteristics of *C. alienum*. a Front views of 6-d-old MEA culture. b Back views of culture. c-d Conidia. e-f Conidiophores. g-i Appressoria. a-i Isolate FYJ-11. Scale bars = 10 μm.

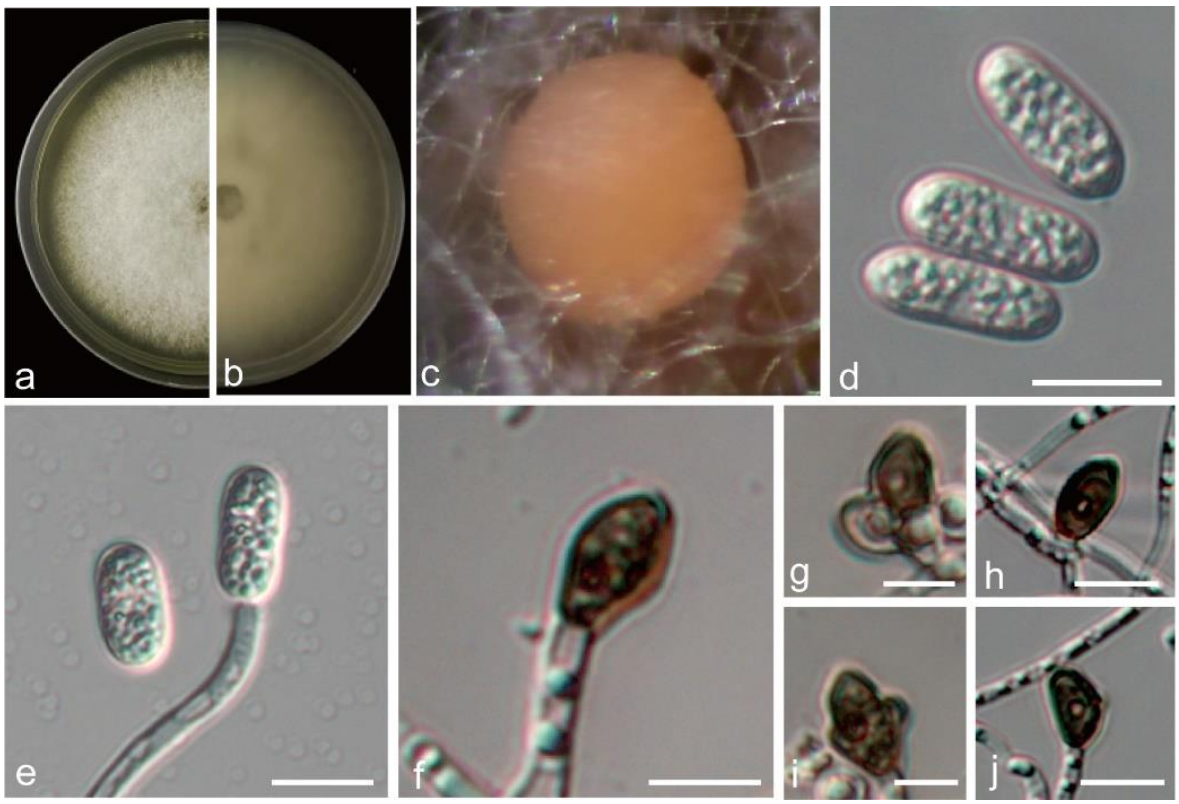

Figure 8 – Morphological characteristics of *C. boninense*. a Front views of 6-d-old MEA culture. b Back views of culture. c Conidiomata. d Conidia. e Conidiophores. f-j Appressoria. Scale bars: d-j = 10 μm, c = 200 μm.

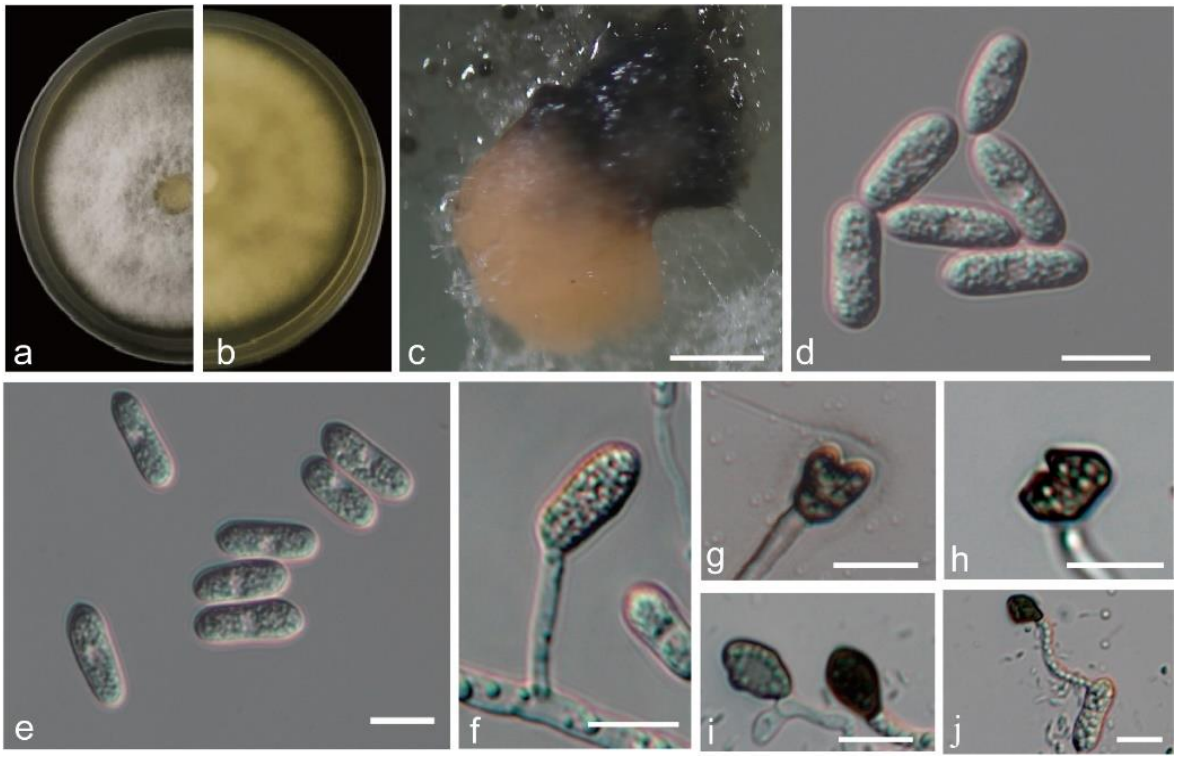

Figure 9 – Morphological characteristics of *C. camelliae.* a Front views of 6-d-old MEA culture. b Back views of culture. c Conidiomata. d-e Conidia. f Conidiophores. g-j Appressoria. a-j Isolate JXJ-20. Scale bars: d-j = 10 μm, c = 200 μm.

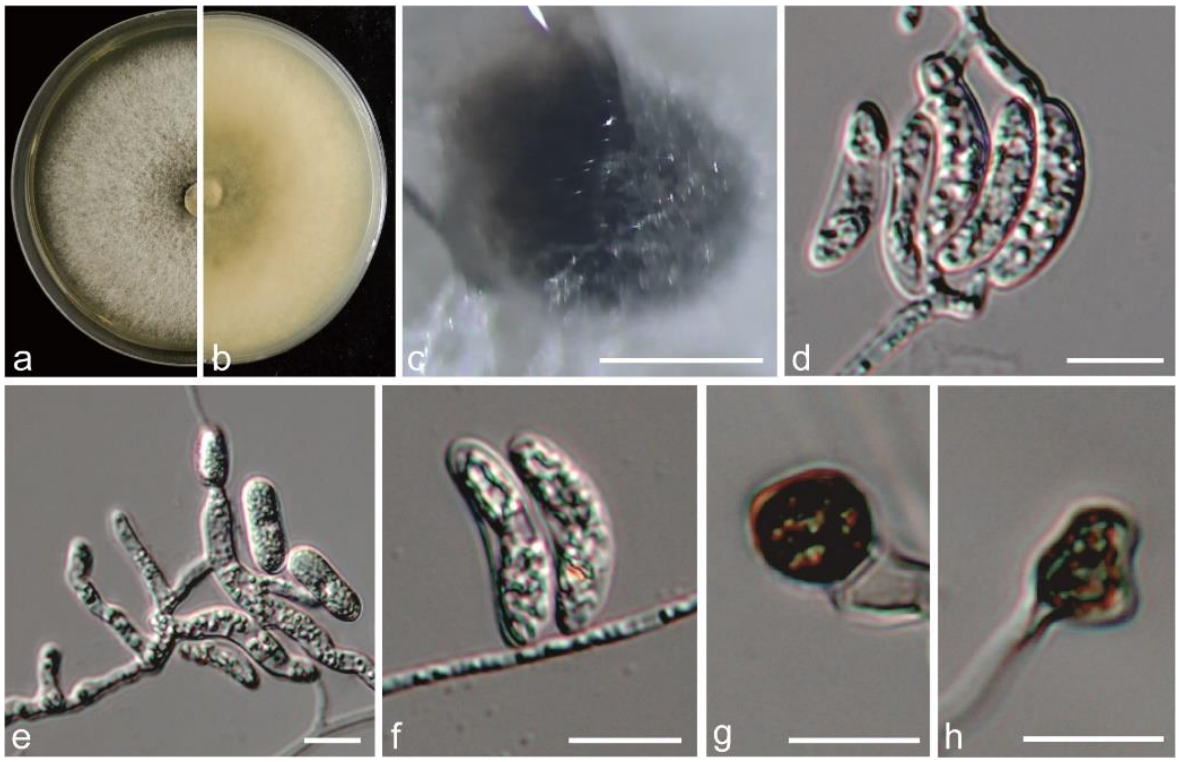

Figure 10 – Morphological characteristics of *C. clivicola.* a Front views of 6-d-old MEA culture. b Back views of culture. c Ascomata. d Conidia. e-f Conidiophores. g-h Appressoria. a-h Isolate SHJ-58. Scale bars: d-h = 10 μm, c = 200 μm.

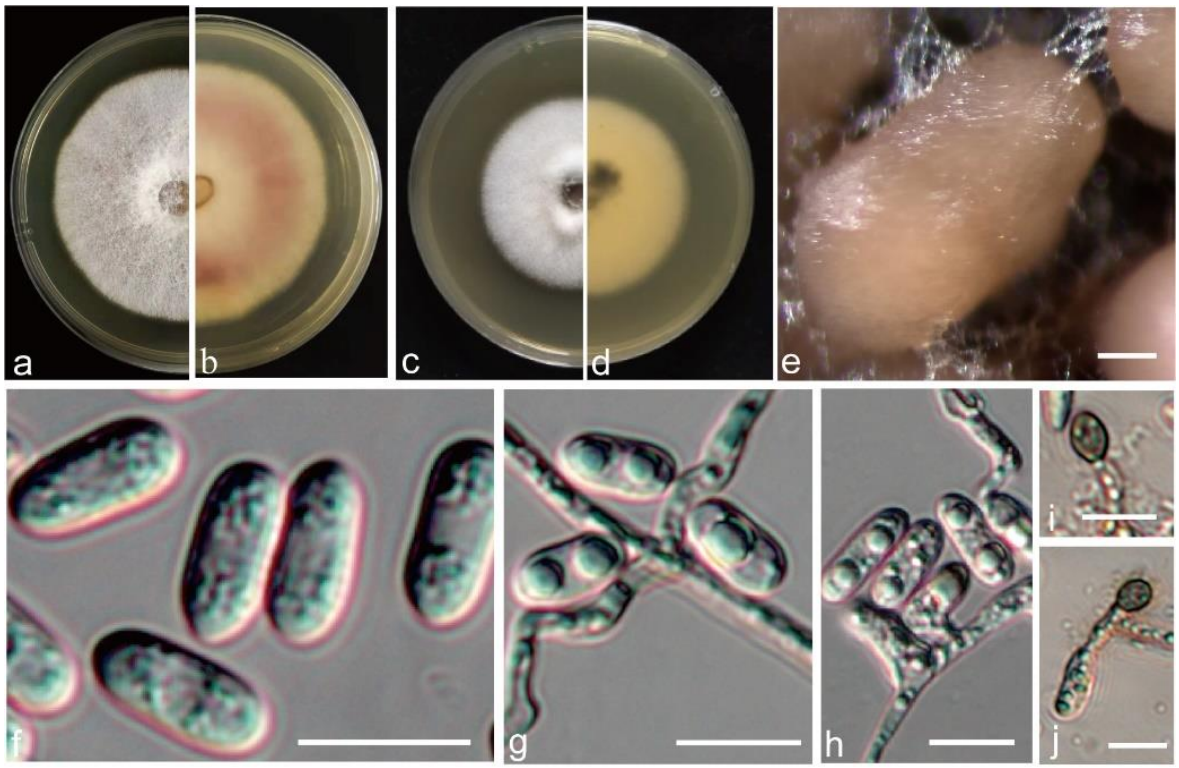

Figure 11 – Morphological characteristics of *C. fioriniae.* a, c Front views of 6-d-old MEA culture. b, d Back views of culture. e Conidiomata. f Conidia. g-h Conidiophores. i-j Appressoria. a-b, e, h Isolate YNJ-1. c-d, f-g, i-j Isolate DJO-36. Scale bars: f-j = 10 μm, e = 200 μm.

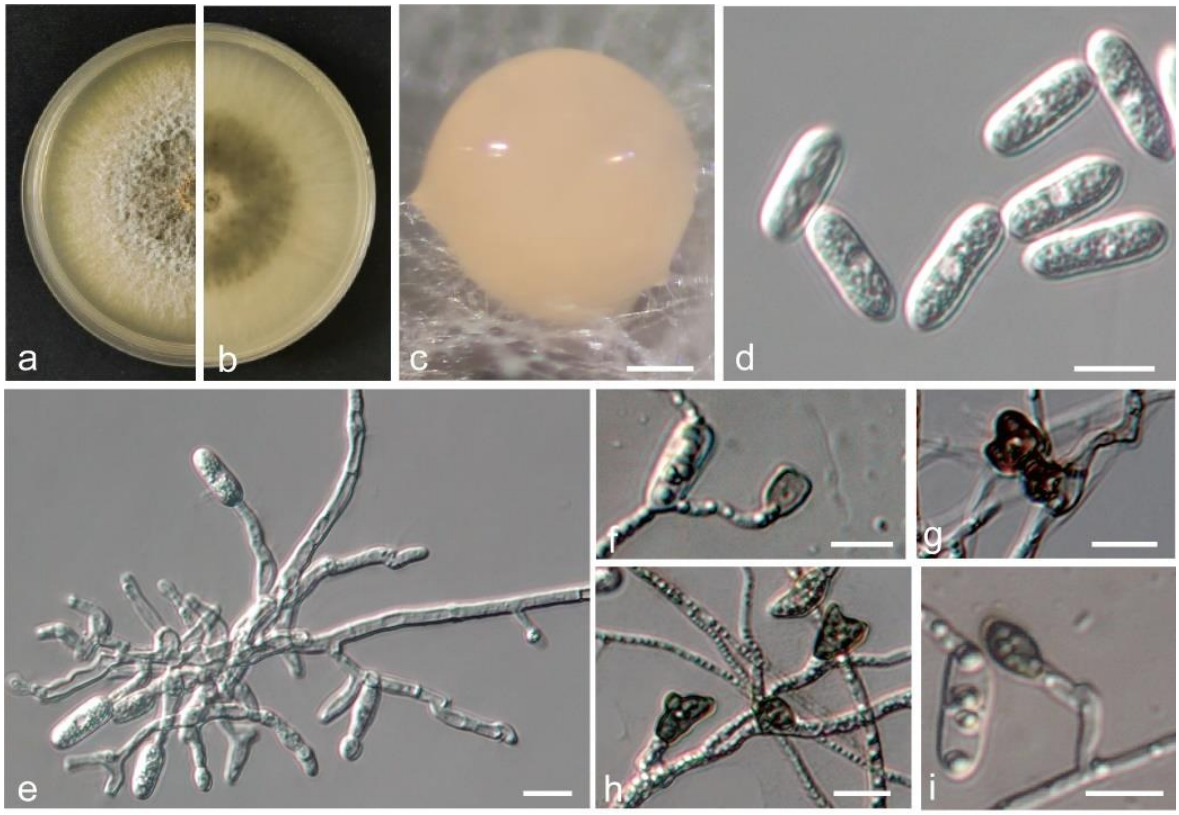

Figure 12 – Morphological characteristics of *C. fructicola.* a Front views of 6-d-old MEA culture. b Back views of culture. c Conidiomata. d Conidia. e Conidiophores. f-i Appressoria. a-i Isolate LAS-24. Scale bars: d-i = 10 μm, c = 200 μm.

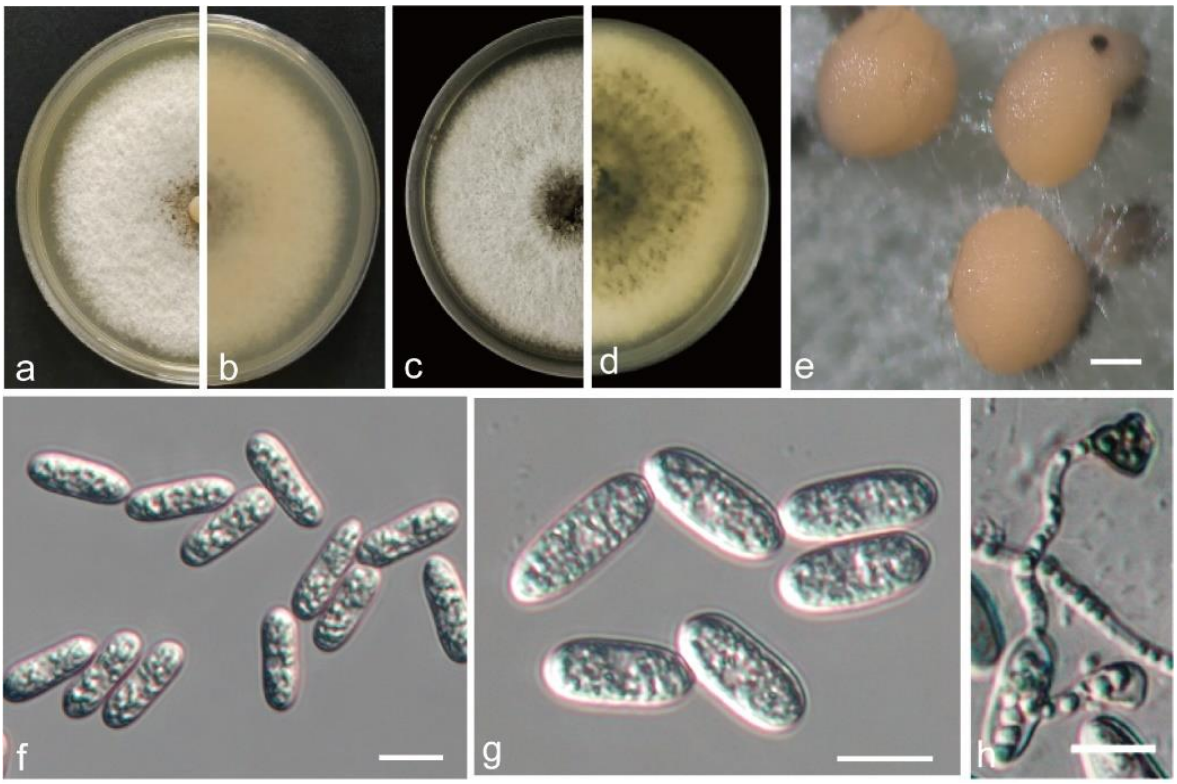

Figure 13 – Morphological characteristics of *C. gloeosporioides*. a, c Front views of 6-d-old MEA culture. b, d Back views of culture. e Conidiomata. f-g Conidia. h Appressoria. a-b, e, f Isolate LAJ-6. c-d, g-h LAS-6. Scale bars: f-h = 10 μm, e = 200 μm.

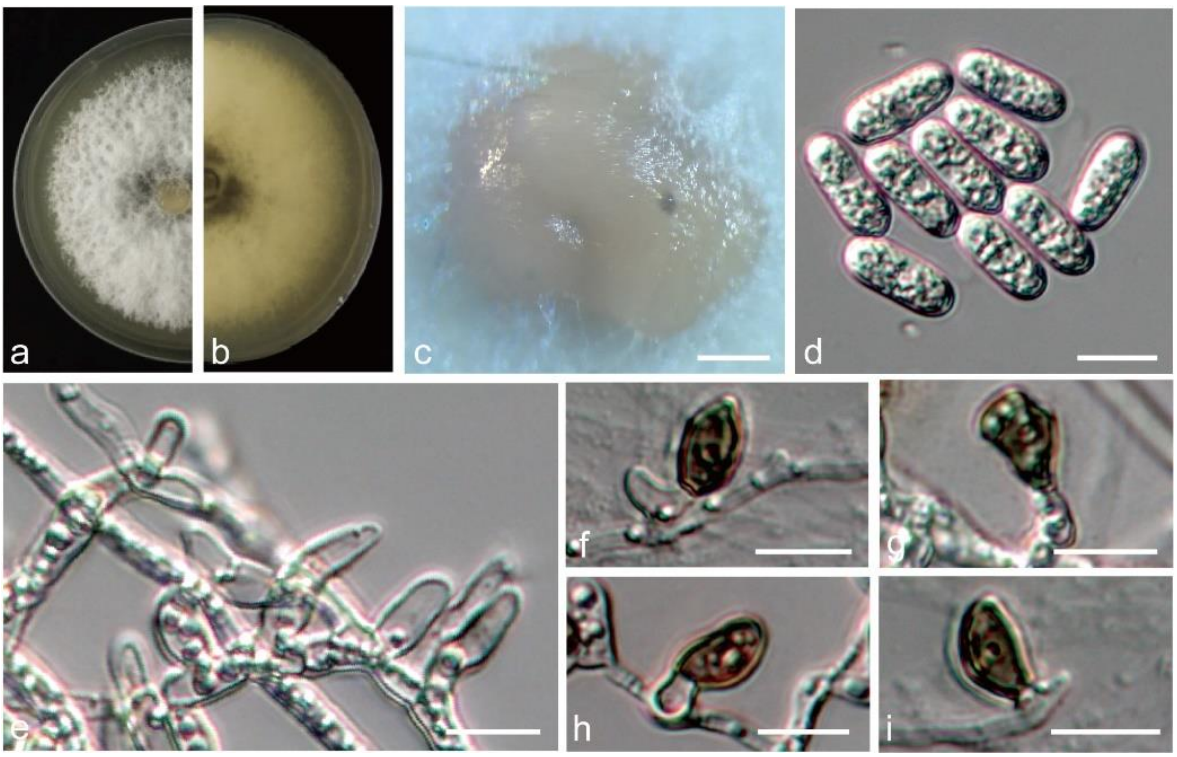

Figure 14 – Morphological characteristics of *C. jiangxiense*. a Front views of 6-d-old MEA culture. b Back views of culture. c Conidiomata. d Conidia. e Conidiophores. f-i Appressoria. a-i Isolate YNJ-17. Scale bars: d-i = 10 μm, c = 200 μm.

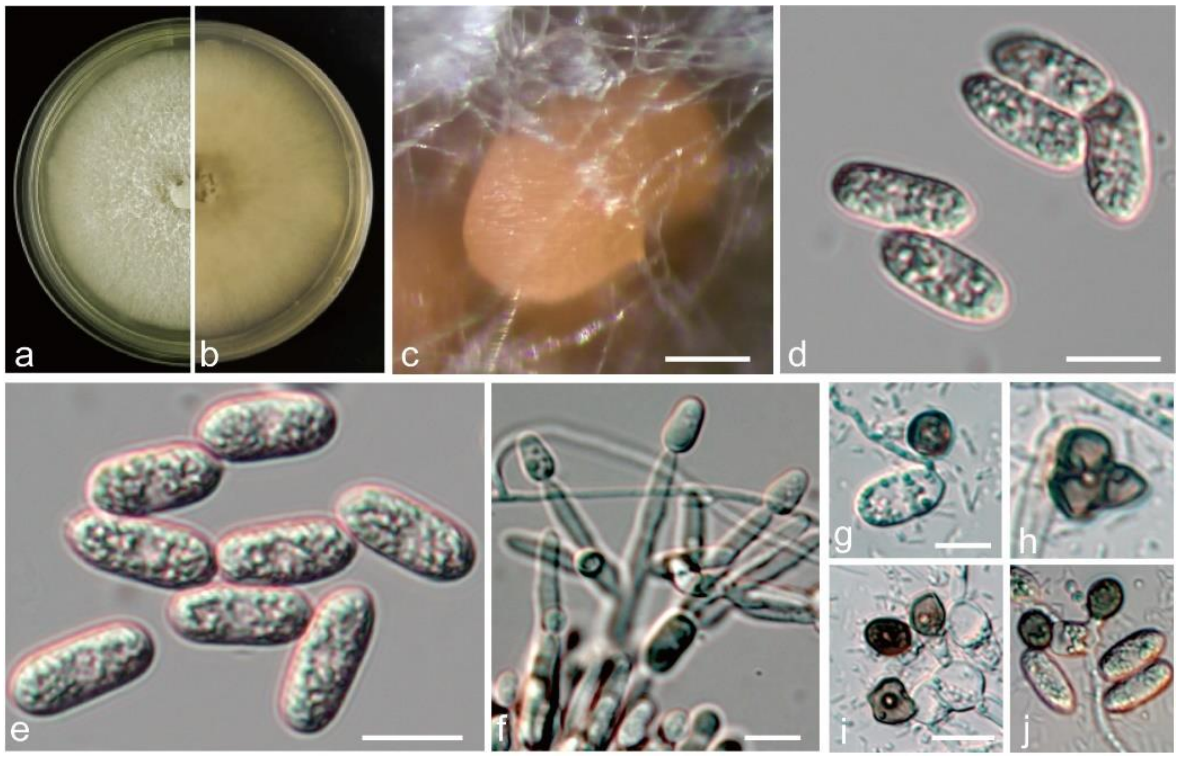

Figure 15 – Morphological characteristics of *C. karstii*. a Front views of 6-d-old MEA culture. b Back views of culture. c Conidiomata. d-e Conidia. f Conidiophores. g-j Appressoria. a-j Isolate YNS-32. Scale bars: d-j = 10 μm, c = 200 μm.

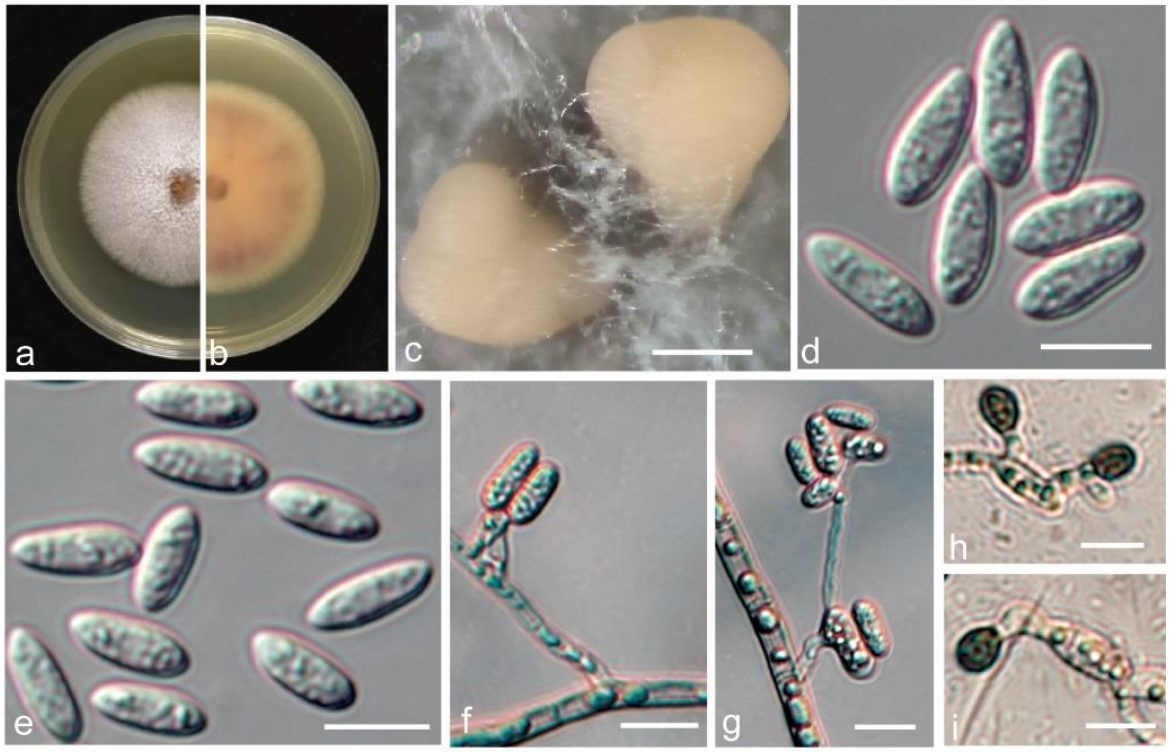

Figure 16 – Morphological characteristics of *C. nymphaeae*. a Front views of 6-d-old MEA culture. b Back views of culture. c Conidiomata. d-e Conidia. f-g Conidiophores. h-i Appressoria. a-i Isolate YNS-42. Scale bars: d-i = 10 μm, c = 200 μm.

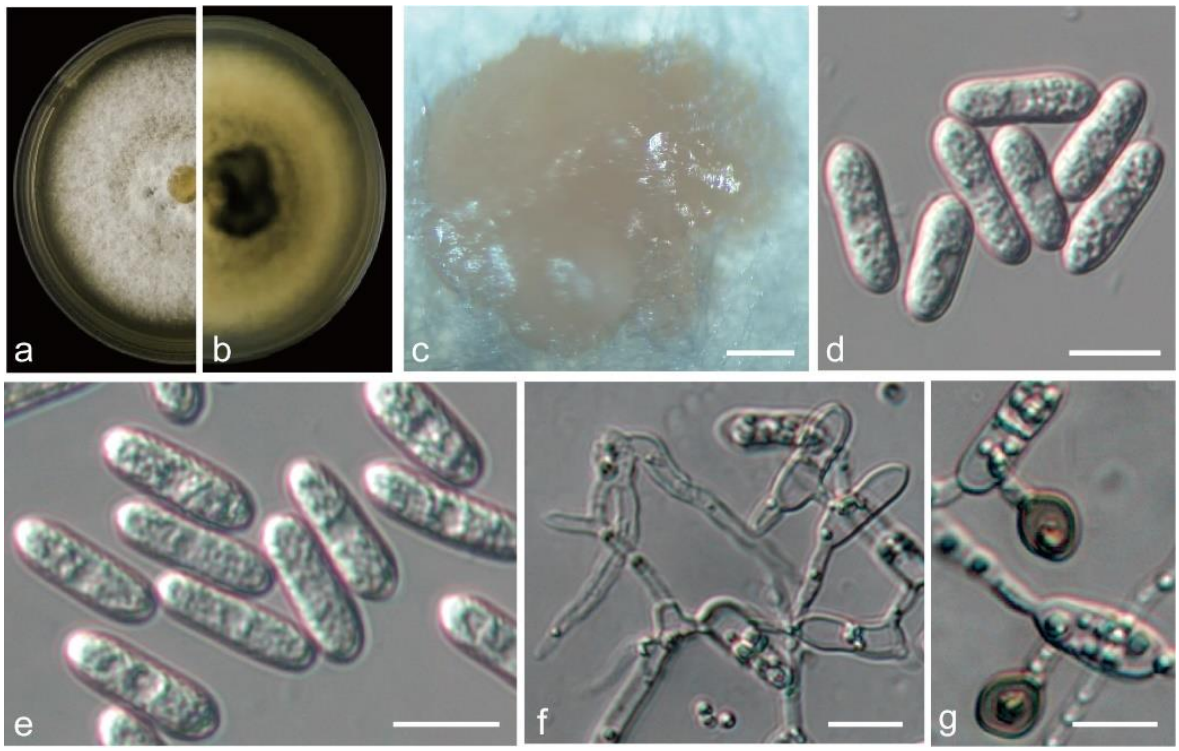

Figure 17 – Morphological characteristics of *C. pandanicola.* a Front views of 6-d-old MEA culture. b Back views of culture. c Conidiomata. d-e Conidia. f Conidiophores. g Appressoria. a-g Isolate SHJ-65. Scale bars: d-g = 10 μm, c = 200 μm.

Figure 18 – Morphological characteristics of *C. plurivorum.* a Front views of 6-d-old MEA culture. b Back views of culture. c Conidiomata. d Conidia. e-f Conidiophores. g-i Appressoria. a-i Isolate YNS-6. Scale bars: d-i = 10 μm, c = 200 μm.

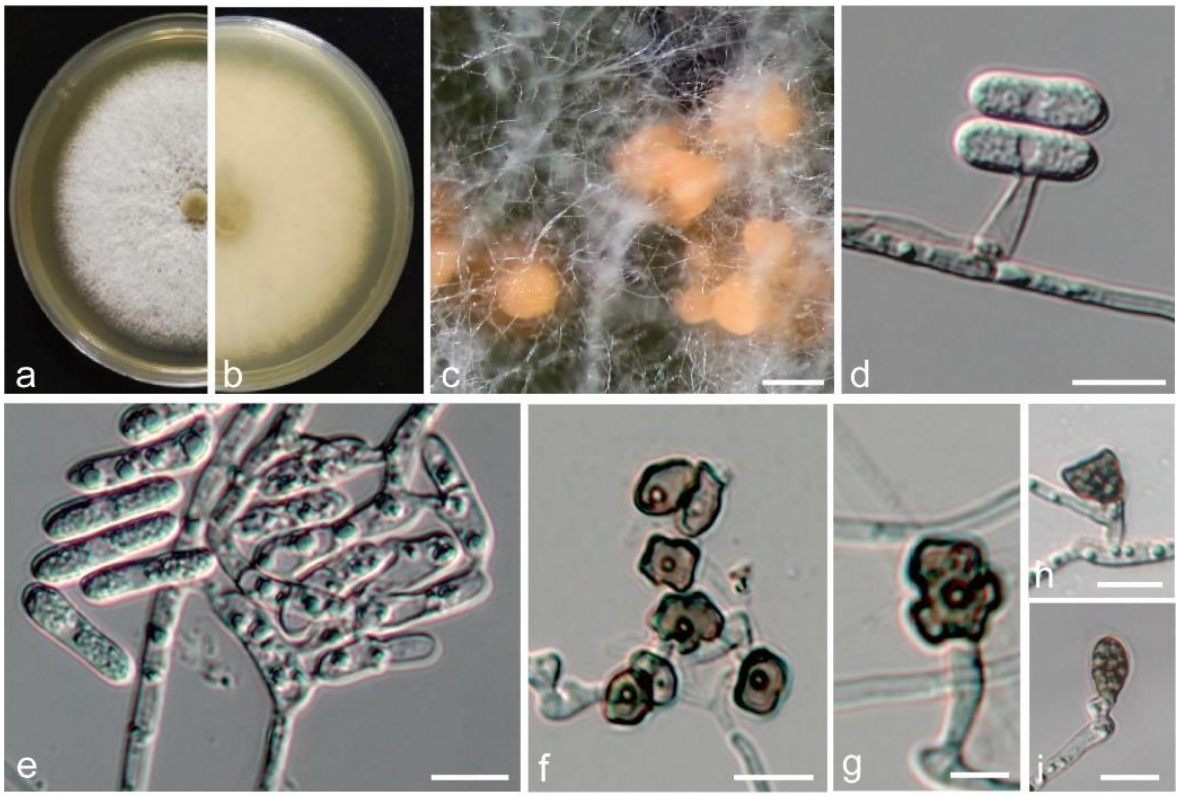

Figure 19 – Morphological characteristics of *C. puerense*. a Front views of 6-d-old MEA culture. b Back views of culture. c Conidiomata. d Conidiophores. e Conidia. f-i Appressoria. a-i Isolate YNS-22. Scale bars: d-i = 10 μm, c = 200 μm.

Figure 20 – Morphological characteristics of *C. siamense*. a, c Front views of 6-d-old MEA culture. b, d Back views of culture. e Conidiomata. f Conidia. g Conidiophores. h-k Appressoria. a-b, e, i Isolate LAJ-20. c-d, f-h, j-k Isolate FYO-85. Scale bars: f-k = 10 μm, e = 200 μm.

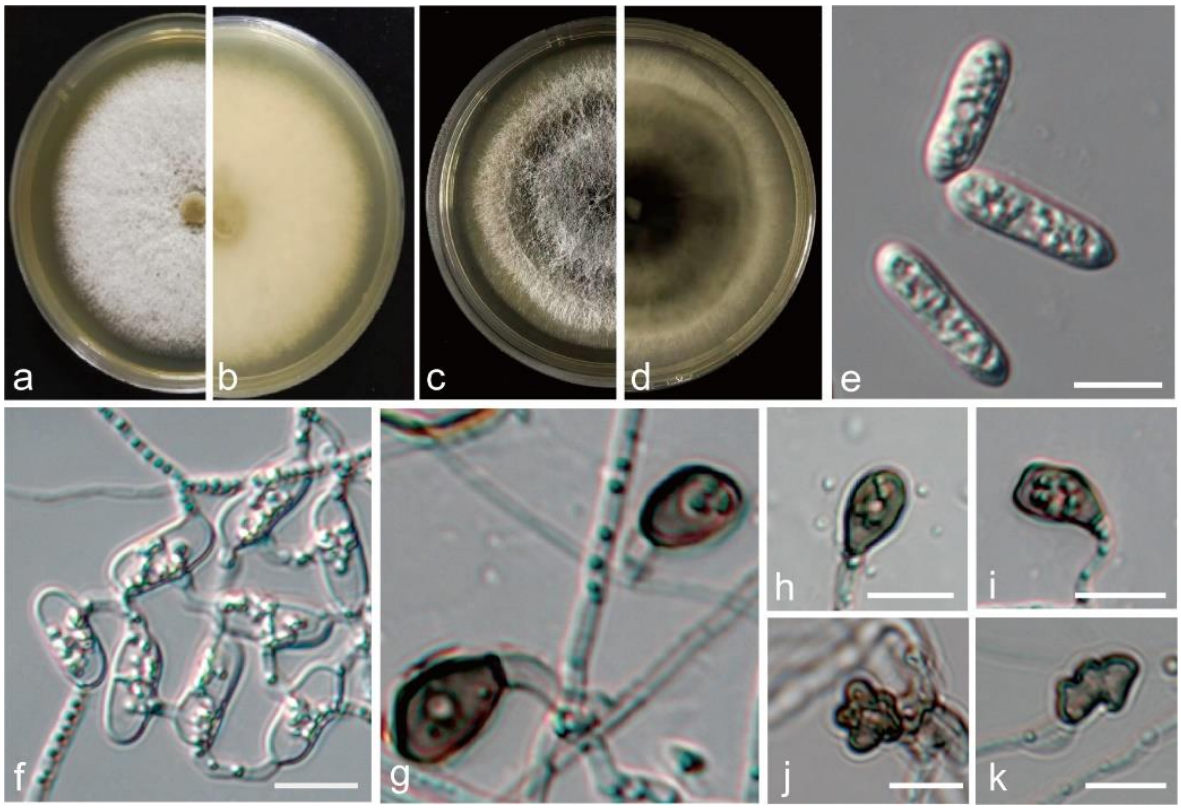

Figure 21 – Morphological characteristics of *C. wuxiense.* a, c Front views of 6-d-old MEA culture. b, d Back views of culture. e Conidia. f Conidiophores. g-k Appressoria. a-b, e-i Isolate LAJ-14. c-d, j-k Isolate DJO-82. Scale bars: e-k = 10 μm.

Table 4 Morphology and lesion lengths of *Colletotrichum* causing on *Camellia* plants.

Species	**Conidial size**	**Mycelial growth diameter (mm/day)**	***Ca. oleifera* Lesion diameter on leaves (mm)**	***Ca. sinensis* Lesion diameter on leaves (mm)**	***Ca. japonica* Lesion diameter on leaves (mm)**
C. aenigma	16.5 ± 0.5 × 5.1 ± 0.3	9.6 ± 0.4 ab	21.5 ± 2.5 b	2.6 ± 0.1 de	2.6 ± 0.6 de
C. alienum	16.0 ± 1.2 × 5.2 ± 0.7	10.7 ± 0.6 ab	5.1 ± 2.0 cd	2.0 ± 0.4 de	1.8 ± 0.2 de
C. camelliae	16.1 ± 1.5 × 5.3 ± 0.5	8.9 ± 0.4 ab	25.7 ± 3.7 a	3.3 ± 1.2 de	4.4 ± 1.1 cde
C. fructicola	17.2 ± 1.3 × 6.2 ± 0.8	10.6 ± 0.6 ab	3.6 ± 1.0 a	2.3 ± 0.1 de	2.2 ± 0.7 de
C. gloeosporioides	16.8 ± 0.5 × 6.3 ± 0.5	11.9 ± 0.4 a	2.6 ± 1.5 de	1.5 ± 0.1 de	2.3 ± 0.3 de
C. jiangxiense	15.2 ± 1.2 × 5.2 ± 0.5	9.9 ± 0.5 ab	7.3 ± 2.1 c	1.6 ± 0.1 de	1.8 ± 0.1 de
C. pandanicola	16.5 ± 0.8 × 5.2 ± 0.4	10.5 ± 0.3 ab	2.0 ± 0.2 de	1.3 ± 0.1 de	2.0 ± 0.5 de
C. siamense	16.2 ± 0.7 × 5.9 ± 0.6	11.0 ± 0.9 ab	2.3 ± 0.4 de	2.5 ± 0.7 de	1.6 ± 0.2 de
C. wuxiense	16.9 ± 1.1 × 5.5 ± 0.2	10.5 ± 0.2 ab	1.9 ± 0.6 de	1.7 ± 0.2 de	2.8 ± 0.4 de
C. puerense	19.1 ± 1.8 × 4.6 ± 0.6	10.2 ± 0.5 ab	1.7 ± 0.1 de	2.0 ± 0.1 de	2.3 ± 0.3 de
C. fioriniae	15.5 ± 1.2 × 5.2 ± 0.7	8.3 ± 0.4 b	3.1 ± 0.1 de	2.1 ± 0.2 de	2.4 ± 0.1 de
C. nymphaeae	13.8 ± 1.1 × 6.0 ± 0.6	8.2 ± 1.0 b	2.5 ± 0.4 de	2.2 ± 0.3 de	2.8 ± 0.6 de
C. boninense	12.5 ± 1.2 × 7.0 ± 0.4	10.2 ± 0.5 ab	2.0 ± 0.3 de	1.9 ± 0.1 de	1.7 ± 0.1 de
C. karstii	14.5 ± 0.8 × 7.0 ± 0.5	9.8 ± 0.4 ab	1.7 ± 0.3 de	1.8 ± 0.2de	1.6 ± 0.1 de
C. clivicola	13.5 ± 0.8 × 6.0 ± 0.7	9.8 ± 0.3 ab	1.9 ± 0.1 de	1.4 ± 0.1 e	2.0 ± 0.2 de
C. plurivorum	18.0 ± 1.2 × 5.8 ± 0.7	10.1 ± 0.6 ab	2.3 ± 0.5 de	1.5 ± 0.1 de	1.9 ± 0.1 de

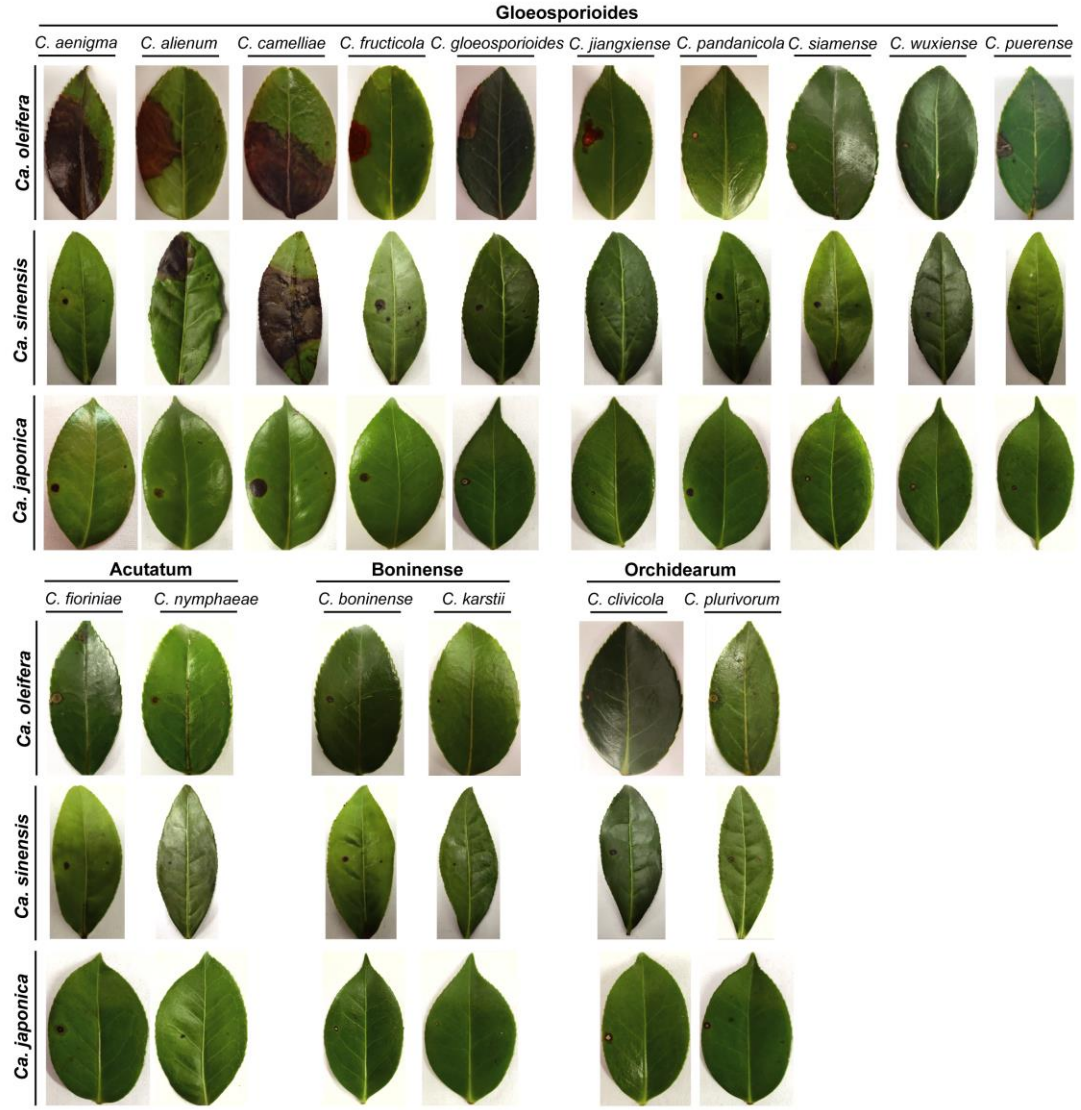

Figure 22 – Symptoms of 16 *Colletotrichum* species inoculated on leaves of *Ca. oleifera*, *Ca. sinensis* and *Ca. japonica* at 14th day.

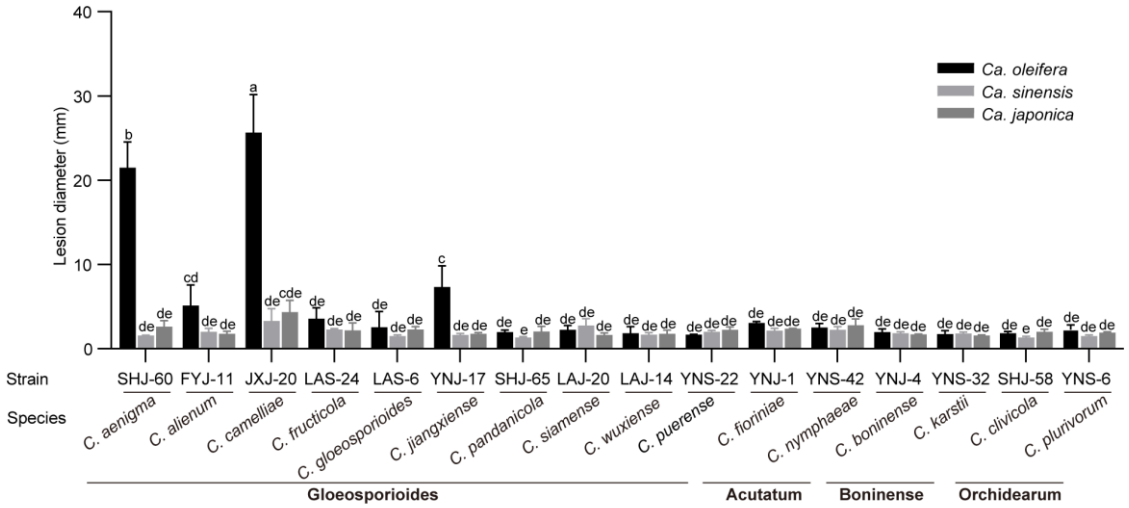

Figure 23 – Lesion diameters on *Ca. oleifera*, *Ca. sinensis* and *Ca. japonica* leaves of 16 *Colletotrichum* species at 14th day after inoculation. Letters over the error bars indicate a significant difference at the $p = 0.05$ level.

Discussion

In this study, we employed morphological and multi-locus phylogenetic analyses to identify the *Colletotrichum* species associated with anthracnose from three important *Camellia* species in China. In total, we obtained a number of 167 isolates residing in four *Colletotrichum* species complexes including *C. gloeosporioides*, *C. acutatum*, *C. boninense*, and *C. orchidearum.* They represent 16 taxa with a newly described species, *C. puerense.* Our study further confirmed that species of *C. aenigma*, *C. alienum*, *C. boninense*, *C. camelliae*, *C. clivicola*, *C. fioriniae*, *C. fructicola*, *C. gloeosporioides*, *C. jiangxinse*, *C. karstii*, *C. nymphaeae*, *C. pandanicola* and *C. wuxiense* can cause *Ca. japonica* anthracnose.

Species in the *C. gloeosporioides* complex such as *C. fructicola*, *C. siamense*, *C. camelliae* were most predominantly isolated from three *Camellia* plants. This is consistent with the previous studies of tea and tea-oil trees anthracnose (Liu et al. 2015, Zhu et al. 2015, Wang et al. 2016, Sun et al. 2021, Zhang et al. 2021). Other studies also revealed that *C. gloeosporioides* complex is the causal agent of anthracnose on a wide range of subtropical and tropical agricultural crops and tree species such as coffee, peach, pear, and chili (Liu et al. 2013, Cao et al. 2019, Jayawardena et al. 2020, Shi et al. 2021, Bhunjun et al. 2022, Tan et al. 2022). The broad host and geographic distribution of this *Colletotrichum* complex might be due to their higher genetic diversity to adopt to changing environmental conditions (McDonald & Linde 2002). The *C. acutatum* complex is the second major pathogen group confirmed from the present study. *Colletotrichum fioriniae* was obtained from three *Camellia* species with five isolates from *Ca. oleifera*, six from *Ca. japonica* and one from *Ca. sinensis*. The second species in the complex *C. nymphaeae* was isolated from *Ca. japonica* (one isolate) and *Ca. sinensis* (two isolates). Further, six isolates in *C. boinense* complex and three isolates in the *C. orchidearum* complex associated with *Ca. sinensis* and *Ca. japonica* anthracnose were identified. It is worth noting that *C. acutatum* and *C. gloeosporioides* complexes were recognized as frequently occurring endophytic fungi in *Camellia* (McDonald & Linde 2002, Liu et al. 2015). This implies that the members of these *Colletotrichum* complexes in *Camellia* may be converted from endophytes to pathogens (Carroll 1988, Wheeler et al. 2019). More importantly, the study described a previously unknown taxon causing *Camellia* anthracnose, namely *C. puerense* from *Ca. sinensis* in Yunnan province. The possible reason is that the various climate environment there might be helpful promoting species diversity (Yang et al. 2004, Liu et al. 2021, Bhunjun et al. 2022).

Pathogenicity test using 16 representative *Colletotrichum* isolates of each obtained species showed that all species were pathogenic, and significant differences existed. Pathogenicity of *C. camelliae* JXJ-20, *C. aenigma* SHJ-60, *C. alienum* FYJ-11 were significantly stronger than other *Colletotrichum* species on three *Camellia* hosts. This is consistent with the previous results demonstrating that *C. camellia* has strong pathogenicity on different plant hosts (Wang et al. 2016, Wang et al. 2020, Zhang et al. 2021). In our study, the pathogenicity of *C. camelliae* JXJ-20 to three plant hosts varied significantly. Species of *C. aenigma* SHJ-60, *C. alienum* FYJ-11, *C. jiangxiense* YNJ-17 were more pathogenic to *Ca. oleifera* while *C. pandanicola* SHJ-65 and *C. clivicola* SHJ-58 were least pathogenic to *Ca. sinensis*. The reasons behind this could be the differences in host resistance and fungal biological characters. Further, only one variety of each host plant was used and it is not enough to fully reflect the actual condition (Mo et al. 2018). Additional research using more genetic clones should be conducted to assess the pathogenicity of the pathogens.

In summary, this represents the first comprehensive investigation of *Colletotrichum* species occurring on three important plant species of *Camellia*, especially those from *Ca. japonica*. A total number of 16 *Colletotrichum* species were characterized and dominant taxa were determined. Our result disclosed that these fungal taxa are pathogenic to three plant hosts, and their pathogenicity varied. The knowledge gained and the diversity of *Colletotrichum* species in *Camellia* gathered provides a useful clue for resistant-germplasm selection and disease management.

Acknowledgements

This study was supported by the Launching Funds for Talents of Zhejiang A & F University (2020FR036), China.

References

Aiello D, Carrieri R, Guarnaccia V, Vitale A et al. 2015 – Characterization and Pathogenicity of *Colletotrichum gloeosporioides* and *C. karstii* Causing Preharvest Disease on *Citrus sinensis* in Italy. Journal of Phytopathology 163, 168–177.

Anand J, Upadhyaya B, Rawat P, Rai N. 2015 – Biochemical characterization and pharmacognostic evaluation of purified catechins in green tea (*Camellia sinensis*) cultivars of India. 3 Biotech 5(3), 285–294.

Bhunjun CS, Phillips AJL, Jayawardena RS, Promputtha I et al. 2021 – Importance of molecular data to identify fungal plant pathogens and guidelines for pathogenicity testing based on Koch's Postulates. Pathogens 10(9): 1096.

Bhunjun CS, Niskanen T, Suwannarach N, Wannathes N et al. 2022 – The numbers of fungi: are the most speciose genera truly diverse?. Fungal Diversity 114(1), 387–462.

Cannon PF, Damm U, Johnston PR, Weir BS. 2014 – *Colletotrichum* – current status and future directions. Studies in Mycology 59(1), 129–145.

Cao XR, Xu XM, Che HY, West JS, Luo DQ. 2019 – Characteristics and distribution of *Colletotrichum* species in coffee plantations in Hainan, China. Plant Pathology 68(6), 1146–1156.

Carbone I, Kohn LM. 1999 – A Method for Designing Primer Sets for Speciation Studies in Filamentous Ascomycetes. Mycologia 91(3), 553–556.

Carroll G. 1988 – Fungal Endophytes in Stems and Leaves: From Latent Pathogen to Mutualistic Symbiont. Ecology 69(1), 2–9.

Chen XG, Jiang LY, Bao AH, Liu CL et al. 2021 – Molecular Characterization, Pathogenicity and Biological Characterization of *Colletotrichum* Species Associated with Anthracnose of *Camellia yuhsienensis* Hu in China. Forests 12(12), 1712.

Chen JX, Wei YQ, Liu L, Zhang DH et al. 2022 – Identification of *Colletotrichum* species associated with *Camellia oleifera* anthracnose in Yunnan and screening of biocontrol bacteria. Journal of South China Agricultural University 43, 43–53.

Chethana KWT, Manawasinghe IS, Hurdeal VG, Bhunjun CS et al. 2021 – What are fungal species and how to delineate them?. Fungal Diversity 109(1), 1–25.

Cristóbal-Martínez AL, de Jesús Yáñez-Morales M, Solano-Vidal R, Segura-León O, Hernández-Anguiano AM. 2017 – Diversity of *Colletotrichum* species in coffee (*Coffea arabica*) plantations in Mexico. European Journal of Plant Pathology 147(3), 605–614.

Damm U, Cannon PF, Woudenberg JHC, Crous PW. 2012a – The *Colletotrichum acutatum* species complex. Studies in Mycology 73(1), 37–113.

Damm U, Cannon PF, Woudenberg JHC, Johnston PR et al. 2012b – The *Colletotrichum boninense* species complex. Studies in Mycology 73(1), 1–36.

Damm U, Sato T, Alizadeh A, Groenewald JZ, Crous PW. 2019 – The *Colletotrichum dracaenophilum*, *C. magnum* and *C. orchidearum* species complexes. Studies in Mycology 92(5): 1–46.

Dissanayake AJ, Bhunjun CS, Maharachchikumbura S, Liu J. 2020 – Applied aspects of methods to infer phylogenetic relationships amongst fungi. Mycosphere 11(1), 2652–2676.

Dowling M, Peres N, Villani S, Schnabel G. 2020 – Managing *Colletotrichum* on Fruit Crops: A "Complex" Challenge. Plant Disease 104(9), 2301–2316.

Fu M, Crous PW, Bai Q, Zhang PF et al. 2019 – *Colletotrichum* species associated with anthracnose of *Pyrus* spp. in China. Persoonia 42(1), 1–35.

Glass NL, Donaldson GC. 1995 – Development of primer sets designed for use with the PCR to amplify conserved genes from filamentous ascomycetes. Applied and Environmental Microbiology 61(4), 1323–1330.
Guarnaccia V, Groenewald JZ, Polizzi G, Crous PW. 2018 – High species diversity in *Colletotrichum* associated with citrus diseases in Europe. Persoonia 39(1), 32–50.
Hou LW, Liu F, Duan WJ, Cai L. 2016 – *Colletotrichum aracearum* and *C. camelliae-japonicae*, two holomorphic new species from China and Japan. Mycosphere 7, 1111–1123.
Huson DH, Bryant D. 2006 – Application of Phylogenetic Networks in Evolutionary Studies. Molecular Biology and Evolution 23(2), 254–267.
Jayawardena RS, Hyde KD, Chen YJ, Papp V et al. 2020 – One stop shop IV: taxonomic update with molecular phylogeny for important phytopathogenic genera: 76–100. Fungal Diversity 103, 87–218.
Jayawardena RS, Hyde KD, de Farias ARG, Bhunjun CS et al. 2021 – What is a species in fungal plant pathogens?. Fungal Diversity 109(1), 239–266.
Katoh K, Standley DM. 2013 – MAFFT multiple sequence alignment software version 7: improvements in performance and usability. Molecular Biology and Evolution 30(4), 772–780.
Kumar S, Stecher G, Tamura K. 2016 – MEGA7: Molecular Evolutionary Genetics Analysis Version 7.0 for Bigger Datasets. Molecular Biology and Evolution 33(7), 1870–1874.
Li L, Li H. 2022 – First report of *Colletotrichum aeschynomenes* causing anthracnose on *Camellia oleifera* in China. Forest Pathology 52(5), e12770.
Li SZ, Li H. 2020 – First Report of *Colletotrichum nymphaeae* Causing Anthracnose on *Camellia oleifera* in China. Plant Disease 104, 1860–1860.
Lin CY, Chen SY, Lee WT, Yen GC. 2022 – Immunomodulatory effect of camellia oil (*Camellia oleifera* Abel.) on CD19 + B cells enrichment and IL-10 production in BALB/c mice. Journal of Functional Foods 88, 104863.
Liu F, Damm U, Cai L, Crous PW. 2013 – Species of the *Colletotrichum gloeosporioides* complex associated with anthracnose diseases of Proteaceae. Fungal Diversity 61(1), 89–105.
Liu F, Hu JM, Yang FL, Li XW. 2021 – Heterogeneity-diversity Relationships in Natural Areas of Yunnan, China. Chinese Geographical Science 31(3), 506–521.
Liu F, Ma ZY, Hou LW, Diao YZ et al. 2022 – Updating species diversity of *Colletotrichum*, with a phylogenomic overview. Studies in Mycology 101, 1–86.
Liu F, Weir BS, Damm U, Crous PW et al. 2015 – Unravelling *Colletotrichum* species associated with *Camellia*, employing ApMat and GS loci to resolve species in the *C. gloeosporioides* complex. Persoonia 35, 63–86.
Liu J, He LI, Zhou G. 2009 – Specific and Rapid Detection of *Camellia oleifera* Anthracnose Pathogen by Nested-PCR. African Journal of Biotechnology 8(6), 1056–1061.
McDonald BA, Linde C. 2002 – The population genetics of plant pathogens and breeding strategies for durable resistance. Euphytica 124(2), 163–180.
Mo J, Zhao G, Li Q, Solangi GS et al. 2018 – Identification and Characterization of *Colletotrichum* Species Associated with Mango Anthracnose in Guangxi, China. Plant Disease 102(7), 1283–1289.
Moon SH, Kim MY. 2018 – Phytochemical profile, antioxidant, antimicrobial and antipancreatic lipase activities of fermented *Camellia japonica* L leaf extracts. Tropical Journal of Pharmaceutical Research 17(5), 905–912.
O'Donnell K, Cigelnik E. 1997 – Two divergent intragenomic rDNAITS2 types within a monophyletic lineage of the fungus *Fusarium* are nonorthologous. Molecular Phylogenetics and Evolution 7, 103–116.
Orrock JM, Rathinasabapathi B, Spakes Richter B. 2019 – Anthracnose in U.S. Tea: Pathogen Characterization and Susceptibility Among Six Tea Accessions. Plant Disease 104(4), 1055–1059.

Peng XJ, Yuan YX, Zhang SK, Zhou XD. 2022 – First Report of Anthracnose on *Camellia japonica* Caused by *Colletotrichum siamense* in Zhejiang Province, China. Plant Disease 106(2), 768.
Quaedvlieg W, Binder M, Groenewald JZ, Summerell BA et al. 2014 – Introducing the Consolidated Species Concept to resolve species in the Teratosphaeriaceae. Persoonia 33, 1–40.
Quan W, Wang A, Gao C, Li C. 2022 – Applications of Chinese *Camellia oleifera* and its By-Products: A Review. Frontiers in Chemistry 10, 921246.
Senanayake IC, Bhat DJ, Cheewangkoon R, Xie N. 2020 – *Bambusicolous Arthrinium* species in Guangdong province, China. Frontiers in Microbiology 11:602773.
Shi NN, Ruan HC, Jie YL, Chen FR, Du YX. 2021 – Characterization, fungicide sensitivity and efficacy of *Colletotrichum* spp. from chili in Fujian, China. Crop Protection 143, 105572.
Sun W, Huang S, Xia J, Zhang X, Li Z. 2021 – Morphological and molecular identification of *Diaporthe* species in south-western China, with description of eight new species. MycoKeys 77, 65–95.
Tan Q, Schnabel G, Chaisiri C, Yin LF et al. 2022 – *Colletotrichum* Species Associated with Peaches in China. Journal of Fungi 8(3), 313.
Talhinhas P, Baroncelli R. 2021 – *Colletotrichum* species and complexes: geographic distribution, host range and conservation status. Fungal Diversity 110, 109–198.
Teixeira AM, Sousa C. 2021 – A Review on the Biological Activity of *Camellia* Species. Molecules 26(8), 2178.
Templeton MD, Rikkerink EH, Solon SL, Crowhurst RN. 1992 – Cloning and molecular characterization of the glyceraldehyde-3-phosphate dehydrogenase-encoding gene and cDNA from the plant pathogenic fungus *Glomerella cingulata*. Gene 122(1), 225–230.
Van der AA HA. 1978 – A leaf spot disease of *Nymphaea alba* in the Netherlands. European Journal of Plant Pathology 84, 109–115.
Wang YC, Hao XY, Wang L, Bin X et al. 2016 – Diverse *Colletotrichum* species cause anthracnose of tea plants (*Camellia sinensis* (L.) O. Kuntze) in China. Scientific Reports 6, 35287.
Wang Y, Chen JY, Xu X, Cheng J et al. 2020 – Identification and Characterization of *Colletotrichum* Species Associated with Anthracnose Disease of *Camellia oleifera* in China. Plant Disease 104, 474–482.
Weir BS, Johnston PR, Damm U. 2012 – The *Colletotrichum gloeosporioides* species complex. Studies in Mycology 73, 115–180.
Wheeler DL, Dung JKS, Johnson DA. 2019 – From pathogen to endophyte: an endophytic population of *Verticillium dahliae* evolved from a sympatric pathogenic population. New Phytologist 222(1), 497–510.
White TJ, Bruns T, Lee S, Taylor J. 1990 – Amplification and direct sequencing of fungal ribosomal rna genes for phylogenetics - ScienceDirect. PCR Protocols, 315–322.
Willis JC. 1899 – DCLII – Tea and coffee diseases. Bulletin of Miscellaneous Information Royal Botanical Gardens Kew 1899: 89–94.
Yang C, Wu P, Yao X, Sheng Y et al. 2022 – Integrated Transcriptome and Metabolome Analysis Reveals Key Metabolites Involved in *Camellia oleifera* Defense against Anthracnose. International Journal of Molecular Sciences 23(1), 536.
Yang S, Wang HX, Yi XJ, Tan LL. 2019 – First report that *Colletotrichum aenigma* causes leaf spots on *Camellia japonica* in China. Plant Disease 103(8), 2127–2128.
Yang KM, Hsu FL, Chen CW, Hsu CL, Cheng MC. 2018 – Quality Characterization and Oxidative Stability of *Camellia* Seed Oils Produced with Different Roasting Temperatures. Journal of Oleo Science 67(4), 389–396.
Yang Y, Tian K, Hao J, Pei S, Yang Y. 2004 – Biodiversity and biodiversity conservation in Yunnan, China. Biodiversity & Conservation 13(4), 813–826.
Yang YL, Cai L, Yu ZN, Liu ZY, Hyde KD. 2011 – *Colletotrichum* species on *Orchidaceae* in southwest China. Cryptogam. Mycology 32, 229–253.

Yang YL, Liu ZY, Cai L, Hyde KD et al. 2009 – *Colletotrichum* anthracnose of Amaryllidaceae. Fungal Diversity 39, 123–146.
Zhang D, Gao F, Jakovlić I, Zou H et al. 2020 – PhyloSuite: An integrated and scalable desktop platform for streamlined molecular sequence data management and evolutionary phylogenetics studies. Molecular Ecology Resources 20(1), 348–355.
Zhang L, Li X, Zhou YY, Tan G, Zhang L. 2021 – Identification and Characterization of *Colletotrichum* Species Associated With *Camellia sinensis* Anthracnose in Anhui Province, China. Plant Disease 105, 2649–2657.
Zhang T, Duan XL, Zhan M, Min X. 2018 – Purification, Preliminary Structural Characterization and In Vitro Antioxidant Activity of Polysaccharides from *Camellia japonica* Pollen. Journal of the Chemical Society of Pakistan 40, 581–589.
Zhao DW, Hodkinson TR, Parnell JAN. 2022 – Phylogenetics of global *Camellia* (Theaceae) based on three nuclear regions and its implications for systematics and evolutionary history. Journal of Systematics and Evolution 12837.
Zhou GY, Song GT, He LI. 2007 – Present Situation and Countermeasures to Control *Camellia oleifera* Pest and Disease. journal of central south university of forestry & technology 6, 179–182.
Zhu YZ, Liao WJ, Zou DX, Wu YJ, Deng Y. 2015 – Identification and biological characteristics of the pathogen from *Camellia oleifera* anthracnose in Guangxi. Journal of Plant Protection 42, 382–389.